Published for SISSA by Springer

Received: *December 19, 2023*
Revised: *March 14, 2024*
Accepted: *April 10, 2024*
Published: *May 2, 2024*

Small Schwarzschild de Sitter black holes, the future boundary and islands

Kaberi Goswami and K. Narayan

Chennai Mathematical Institute,
SIPCOT IT Park, Siruseri 603103, India

E-mail: goswamikaberi500@gmail.com, narayan@cmi.ac.in

Abstract: We continue the study of 4-dimensional Schwarzschild de Sitter black holes in the regime where the black hole mass is small compared with the de Sitter scale, following arXiv:2207.10724 [hep-th]. The de Sitter temperature is very low compared with that of the black hole. We consider the future boundary as the location where the black hole Hawking radiation is collected. Using 2-dimensional tools, we find unbounded growth of the entanglement entropy of radiation as the radiation region approaches the entire future boundary. Self-consistently including appropriate late time islands emerging just inside the black hole horizon leads to a reasonable Page curve. We also discuss other potential island solutions which show inconsistencies.

Keywords: 2D Gravity, Black Holes, Effective Field Theories

ArXiv ePrint: 2312.05904

https://doi.org/10.1007/JHEP05(2024)016

Contents

1 Introduction

The black hole information paradox [1] has seen fascinating progress over the last few years: in this context it is perhaps best to regard this, not as a detailed understanding of black hole microstates, but as the tension between the apparent unbounded growth of entanglement entropy of Hawking radiation [2] outside the black hole and the quantum mechanics expectation that entanglement entropy must become small at late times to recover purity of the original matter state (see e.g. [3, 4], which review various aspects of the information paradox). This falling Page curve [5, 6], reflecting the original purity, can be recovered when nontrivial, spatially disconnected, island saddles for quantum extremal surfaces are included [7–11].

Quantum extremal surfaces are extrema of the generalized gravitational entropy [12, 13] obtained from the classical area of the entangling RT/HRT surface [14–17] after incorporating the bulk entanglement entropy of matter. Effective 2-dimensional models allow explicit calculation, where 2-dim CFT techniques enable detailed analysis of the bulk entanglement entropy. The island, arising as a nontrivial solution to extremization (near the black hole horizon, and only at late times), reflects new replica wormhole saddles [10, 11] and serves to purify the early Hawking radiation thereby lowering the entanglement entropy. There is a large body of literature on various aspects of these issues, reviewed in e.g. [18–20]: see e.g. [21–122] for a partial list of investigations on black holes in various theories, and also cosmological

JHEP05(2024)016

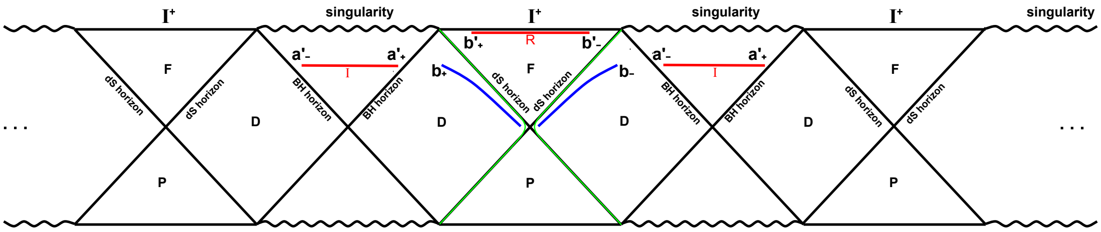

Figure 1. The Penrose diagram of a Schwarzschild de Sitter black hole, with radiation region near the future boundary I^+. Depicted are the radiation regions (blue lines) in the static patches, which are analytically continued to the radiation region $R \equiv [b'_+, b'_-]$ at I^+ and the late time island $I \equiv [a'_-, a'_+]$ on both sides.

contexts. It is important to note that several of these investigations are simply applications of the island proposal, which appears to be self-consistent, even if it cannot be rigorously derived in those contexts (see e.g. [19] for an overall critical perspective, as well as [64, 65] and [66]).

This paper continues the study in [92] of "small" Schwarzschild de Sitter black holes, with the black hole mass m small compared with the de Sitter scale l, but large enough that a quasi-static approximation to the geometry is valid. The de Sitter temperature is very low compared with that of the black hole so the ambient de Sitter space is approximated as a frozen classical background. For calculational purposes, we consider an effective 2-dim dilaton gravity model obtained by dimensional reduction, with the bulk matter representing the black hole Hawking radiation modelled as a 2-dim CFT propagating on this 2-dim space: this is reasonable under the assumption that the s-wave Hawking modes are dominant. We imagine that the black hole has formed from initial matter in a pure state which is a reasonable approximation since the de Sitter temperature is very low (more generally, the bulk matter CFT is in a thermal state at the de Sitter temperature). In [92], we focussed on one black hole coordinate patch in the Penrose diagram (roughly a line of alternating Schwarzschild and de Sitter patches, see figure 1) and considered observers in the static diamond patches far outside the black hole but within the cosmological horizons. While the entanglement entropy of the radiation region exhibits unbounded growth, reflecting the information paradox for the black hole (which has finite entropy), including appropriate island contributions recovers finiteness of entanglement, and thereby expectations on the Page curve. The island emerges at late times a little outside the black hole horizon semiclassically.

The Hawking radiation from the black hole is expected to cross the cosmological horizon and eventually reach the future boundary where it is collected (figure 1). In this paper, we consider the point of view of these future boundary (meta)observers, and look for semiclassical island resolutions of the black hole information paradox with regard to a radiation region at the future boundary. The future boundary is in a sense better defined (compared to the static diamond) as a place where gravity is manifestly weak, the space expanding indefinitely. The radiation region taken as an interval with length labelled by X (alongwith spheres) on the future boundary can be parametrized via Kruskal coordinates T, X, defined by analytic continuation from the static diamond coordinates. We find that the entanglement entropy of Hawking radiation exhibits unbounded growth in the spatial length X along the future boundary, inconsistent with the finiteness of black hole entropy, and reflecting the information paradox. Using the island rule in the extremization of the generalized entropy shows islands emerging for large values of X a little inside the black hole horizon semiclassically: including the island contributions recovers expectations on the Page curve. This future boundary radiation region is entangled with island regions around the horizons of black hole regions on both left and right cosmological horizons (figure 1): this is expected since the future boundary receives Hawking modes from both left and right black holes. Our analysis has some parallels with the island studies in [89] for dS_2 arising under reductions from Nariai limits of higher dim Schwarzschild de Sitter. One might expect timelike separated quantum extremal surfaces for the future boundary resulting in complex-valued entropies as are known in pure de Sitter (see [68] for dS_2, and [86] for reductions of higher dimensional Poincare dS; see also [123–127] for classical RT/HRT surfaces anchored at the future boundary). However Schwarzschild de Sitter has a "sufficiently wide" Penrose diagram so spacelike separated islands do exist here in accordance with physical expectations for the black hole Page curve (thus we discard timelike separated ones here).

In section 2, we review the Schwarzschild de Sitter geometry and discuss parametrizations in various coordinate patches in section 2.1. Section 3 discusses the entanglement entropy without islands (details in appendix B), while section 4 discusses the island calculation (details in appendix C). Appendix A is a brief review of the analysis in [92] for radiation entropy with islands from the point of view of the static diamond observers. Appendix D.1–D.2 discuss inconsistencies in other potential island solutions, while appendix E discusses timelike separated quantum extremal surface solutions for future boundary observers. Section 5 contains a Discussion on various aspects of our study.

2 Small Schwarzschild de sitter black holes → 2-dim

The Schwarzschild de Sitter black hole spacetime in $3+1$-dimensions has the metric

$$ds^2 = -f(r)dt^2 + \frac{dr^2}{f(r)} + r^2 d\Omega_2^2 \,, \qquad f(r) = 1 - \frac{2m}{r} - \frac{r^2}{l^2} \,. \tag{2.1}$$

This is a Schwarzschild black hole in de Sitter space [128] with an "outer" cosmological (de Sitter) horizon and an "inner" Schwarzschild horizon. The general $d+1$-dimensional SdS spacetime is of similar form but with $f(r) = 1 - \frac{2m}{l}(\frac{l}{r})^{d-2} - \frac{r^2}{l^2}$, and will have qualitative parallels. We are focussing on the 4-dim case SdS_4 here: the function $f(r)$ is a cubic and the zeroes of $f(r)$, i.e. solutions to $f(r) = 0$, give the horizon locations. We parametrize this as

$$\begin{gathered} f(r) = 1 - \frac{2m}{r} - \frac{r^2}{l^2} = \frac{1}{l^2 r}(r_D - r)(r - r_S)(r + r_S + r_D)\,, \\ r_D r_S (r_D + r_S) = 2ml^2\,, \qquad r_D^2 + r_D r_S + r_S^2 = l^2\,; \qquad 0 \le r_S \le r_D \le l\,; \qquad \frac{m}{l} \le \frac{1}{3\sqrt{3}}\,. \end{gathered} \tag{2.2}$$

We will take the roots r_S and r_D to label the Schwarzschild black hole and de Sitter (cosmological) horizons respectively. (The third zero $-(r_D + r_S)$ does not correspond to a physical horizon.) The roots r_S, r_D are constrained as above. The case with $m = 0$, or $r_S = 0,\ r_D = l$, is pure de Sitter space, while the flat space Schwarzschild black hole has $r_S = 2m,\ r_D = l,\ l \to \infty$.

JHEP05(2024)016

The surface gravity at both horizons are generically distinct: Euclidean continuations removing a conical singularity can be defined at each horizon separately but not simultaneously at both [129] (see also [130, 131]). The only (degenerate) exception is in an extremal, or Nariai, limit [132] where both periodicities of Euclidean time match: the spacetime develops a nearly dS_2 throat in this extremal limit [129]. More on the nearly dS_2 limit and the wavefunction of the universe appears in [133]. Related discussions with some relevance to this paper also appears in [134]. In more detail, it can be seen that the above horizon structure is valid for $\frac{m}{l} < \frac{1}{3\sqrt{3}}$, beyond which there are no horizons [128]. The limit $\frac{m}{l} = \frac{1}{3\sqrt{3}}$ with the cosmological and Schwarzschild horizon values coinciding, has $r_S = r_D = r_0 = \frac{l}{\sqrt{3}}$ from (2.2): this extremal, or Nariai, limit has a near horizon $dS_2 \times S^2$ throat. Overall the range of physically interesting r_S, r_D satisfies $0 < r_S < r_0 < r_D$ for generic values. The cosmological horizon is "outside" the Schwarzschild one since $r_S < r_D$. The black hole interior has $r < r_S$ with $r \to 0$ the singularity. The region $r_D < r \le \infty$ describes the future and past de Sitter universes, with $r \to \infty$ the future boundary I^+ (or past, I^-). The maximally extended Penrose diagram in figure 1 shows an infinitely repeating pattern of Schwarzschild coordinate patches or "unit-cells" containing Schwarzschild black hole horizons cloaking interior regions: these patches are bounded by cosmological horizons on the left and right, with future/past universes beyond the cosmological horizons.

As in [92], we are considering the limit of a "small" black hole in de Sitter with

$$m \ll l\,, \qquad l \to \text{large} \quad \Rightarrow \quad r_D \gg r_S\,. \tag{2.3}$$

The horizon locations can then be found perturbatively to be $r_S \simeq 2m\,,\ r_D \simeq l - m \gg r_S\,,$ from (2.2). This is a small black hole in a large accelerating universe, so the ambient cosmology is effectively a frozen classical background while the black hole Hawking evaporates. The black hole temperature is much larger than the Gibbons-Hawking de Sitter temperature: from [130, 131] (see also [135]) the surface gravities $\kappa_{\rm BH,dS} = \frac{1}{2\sqrt{f(ml^2)}}|\frac{df}{dr}|_{r_S,r_D}$ become $\frac{1}{2\beta_{S,D}}\frac{1}{\sqrt{1-3(m/l)^{2/3}}}$, with $\beta_{S,D}$ in (2.7). Then the temperatures $T = \frac{\kappa}{2\pi}$ in the limit (2.3) become

$$T_{\rm BH} \sim \frac{1}{8\pi m}\,, \qquad T_{\rm dS} \sim \frac{1}{2\pi l}\,; \qquad\qquad T_{\rm dS} \ll T_{\rm BH}\,. \tag{2.4}$$

The limit of asymptotically flat space is $r_D \sim l \to \infty$, $\frac{r_D}{l} \to 1$, $r_S \to 2m$ and $T_{\rm dS} \to 0$ so the ambient de Sitter temperature vanishes. Our discussions in this paper also pertain to these small Schwarzschild de Sitter black holes.

2.1 Coordinate parametrizations in various coordinate patches

We will describe various coordinate parametrizations in the various coordinate choices in the Schwarzschild de Sitter spacetime, involving Kruskal variables around the black hole horizon and around the cosmological horizon.

In [92], we considered the radiation region to be in the static diamond bounded by the black hole and cosmological horizons in the Schwarzschild de Sitter background: this static patch is parametrized by certain Kruskal coordinates [136] in the vicinity of the black hole horizon. For our present purposes, we would like to analytically extend the Kruskal

JHEP05(2024)016

coordinates (U_D, V_D) defined in the static patch in the vicinity of the cosmological horizon and (U_S, V_S) near the black hole horizon to a new set of Kruskal coordinates (U'_D, V'_D) lying within the future universe, near the future boundary, and (U'_S, V'_S) in the interior of black hole (inside the horizon) respectively. We will first define the set of coordinates in the static patch and then analytically extend them beyond both horizons.

We will first recast the Schwarzschild de Sitter metric (2.1) in the static patch in terms of the Kruskal coordinates which are regular at the cosmological horizon (but not in the vicinity of the black hole horizon). Towards this, we define the tortoise coordinate following [136]:

$$r^* = \int \frac{1}{f(r)}\, dr = \int \frac{1}{1-\frac{2m}{r}-\frac{r^2}{l^2}}\, dr = \int \frac{l^2 r}{(r_D-r)(r-r_S)(r+r_S+r_D)}\, dr\,. \tag{2.5}$$

Taking $f(r)>0$ in the region $r_S<r<r_D$, this gives

$$e^{r^*} = (r_D-r)^{-\beta_D}(r-r_S)^{\beta_s}(r+r_D+r_S)^{\beta_M}\,, \tag{2.6}$$

with the parameters (which simplify dr^*/dr to $1/f(r)$, and satisfy $\beta_M+\beta_S=\beta_D$)

$$\beta_D = \frac{l^2 r_D}{(r_D-r_S)(2r_D+r_S)}\,, \quad \beta_S = \frac{l^2 r_S}{(r_D-r_S)(2r_S+r_D)}\,, \quad \beta_M = \frac{l^2(r_D+r_S)}{(2r_D+r_S)(2r_S+r_D)}\,. \tag{2.7}$$

The SdS_4 metric (2.1) is recast as $ds^2 = f(r)(-dt^2+dr^{*2}) + r^2 d\Omega_2^2$. We label the spacetime coordinates in the left and right regions in the vicinity of the cosmological horizon as

$$b_+ : \quad (t,r) = (t_b, b)\,, \qquad b_- : \quad (t,r) = \left(-t_b+\frac{i\beta}{2}, b\right); \qquad \beta = \frac{2\pi}{\alpha_D}\,. \tag{2.8}$$

This choice of β is simply a convenient way of incorporating the relative minus signs in the Kruskal coordinates in the left and right regions through $e^{i\beta\alpha_D/2} = e^{i\pi} = -1$. In the static patch, in the vicinity of the cosmological horizon, these cosmological Kruskal coordinates U_D, V_D, and the Schwarzschild de Sitter metric become

$$\begin{aligned}
&b_+ : \qquad\qquad U_{D_+} = e^{\alpha_D(t_b-r^*)}\,, \quad V_{D_+} = -e^{-\alpha_D(t_b+r^*)}\,,\\
&\alpha_D = \frac{1}{2\beta_D}\,; \quad U_{D_+}V_{D_+} = -e^{-2\alpha_D r^*}\,, \quad \frac{U_{D_+}}{V_{D_+}} = -e^{2\alpha_D t_b}\,; \quad ds^2 = -\frac{dU_{D_+}dV_{D_+}}{{W_b}^2} + r^2 d\Omega^2\,,\\
&W_b = \sqrt{r}\, l\, \alpha_D (r_D-r)^{-\frac{(1-2\alpha_D\beta_D)}{2}}(r-r_S)^{-\frac{(1+2\alpha_D\beta_S)}{2}}(r+r_S+r_D)^{-\frac{(1+2\alpha_D\beta_M)}{2}}\,.
\end{aligned} \tag{2.9}$$

The value of α_D here ensures regularity at the cosmological horizon. ($\beta_M+\beta_S=\beta_D$ ensures that W has dimensions of inverse length.) With this parametrization of the left and right time coordinates, we conveniently use the expressions in (2.9), with β automatically doing the left-right book-keeping.

We are now considering an interval at the future boundary I^+ where the Hawking radiation from the black hole is expected to be collected. Towards parametrizing this future boundary radiation region, we will analytically continue the cosmological Kruskal coordinates defined above in the static patch to the region beyond the cosmological horizon (i.e. the future universe) keeping invariant, as usual, the metric expressed in terms of the

JHEP05(2024)016

new cosmological Kruskal coordinates beyond the cosmological horizon. Let us consider the analytic continuation in $(t_b, {r_b}^*)$ coordinates as

$$(t_b, {r_b}^*) \rightarrow \left(X_{b'} = \alpha_D \left(t_b - \frac{i\pi}{2\alpha_D} \right), T_{b'} = \alpha_D \left({r_b}^* - \frac{i\pi}{2\alpha_D} \right) \right). \tag{2.10}$$

Thus the new cosmological Kruskal coordinates at both ends b'_+ and b'_- of the future boundary radiation region are defined as (U'_{D_+}, V'_{D_+}) and (U'_{D_-}, V'_{D_-}) respectively and the Schwarzschild de Sitter metric in terms of $(X_{b'}, T_{b'})$ coordinates becomes

$$\begin{aligned}
b'_+ : \quad & U'_{D_+} = e^{(X_{b'} - T_{b'})}, \qquad V'_{D_+} = e^{-(X_{b'} + T_{b'})}, \\
b'_- : \quad & U'_{D_-} = e^{-(X_{b'} + T_{b'})}, \qquad V'_{D_-} = e^{(X_{b'} - T_{b'})}, \\
& U'_{D_\pm} V'_{D_\pm} = e^{-2T_{b'}}, \qquad \frac{U'_{D_\pm}}{V'_{D_\pm}} = e^{\pm 2X_{b'}}; \quad ds^2 = \frac{1}{\alpha_D^2} |f(r)| \left(-dT_{b'}^2 + dX_{b'}^2 \right) + r^2 d\Omega^2, \\
& |f(r)| = \frac{1}{l^2 r} (r - r_D)(r - r_S)(r + r_S + r_D).
\end{aligned} \tag{2.11}$$

The Schwarzschild de Sitter metric now becomes

$$\begin{aligned}
& ds^2 = -\frac{dU'_{D_\pm} dV'_{D_\pm}}{{W_{b'}}^2} + r^2 d\Omega^2, \\
& W_{b'} = \sqrt{r}\, l\, \alpha_D (r - r_D)^{-\frac{(1 - 2\alpha_D \beta_D)}{2}} (r - r_S)^{-\frac{(1 + 2\alpha_D \beta_S)}{2}} (r + r_S + r_D)^{-\frac{(1 + 2\alpha_D \beta_M)}{2}}.
\end{aligned} \tag{2.12}$$

For our purposes, it is a reasonable approximation to look at the s-wave sector of the black hole and consider the bulk matter as a 2-dim CFT: this enables the use of 2-dim CFT tools to study the entanglement entropy of bulk matter. So, we will consider the same dimensional reduction of the 4-dim Schwarzschild de Sitter spacetime to a 2-dim background, as in [92] (see the general reviews [137–139], and [140] for related discussions, as well as [141] for certain families of 2-dim cosmologies).

Recalling from [92], the reduction ansatz $ds^2_{(4)} = g^{(2)}_{\mu\nu} dx^\mu dx^\nu + \lambda^{-2} \phi\, d\Omega_2^2$ alongwith a Weyl transformation $g_{\mu\nu} = \phi^{1/2} g^{(2)}_{\mu\nu}$ to absorb the dilaton kinetic term gives the 2-dim dilaton gravity theory $\frac{1}{16\pi G_2} \int d^2x \sqrt{-g}\, (\phi \mathcal{R} - \frac{6}{l^2} \phi^{1/2} + 2\lambda^2 \phi^{-1/2})$. The lengthscale λ^{-1} makes the dilaton ϕ dimensionless, which then maps to the 4-dim transverse area of 2-spheres $\frac{4\pi\phi}{\lambda^2}$. With G_N the 4-dim Newton constant, $G_2 = \frac{G_N}{V_2}$ and $V_2 = \frac{4\pi}{\lambda^2}$, the 2-dim theory has area term $\frac{\phi}{4G_2} = \frac{4\pi r^2}{4G_N}$ equivalent to the 4-dim one. Our discussion is entirely gravitational so it is reasonable to take the Planck length as the natural UV scale with $\lambda^{-1} \sim \epsilon_{\rm UV} \sim l_P$. So finally, the dilaton is $\phi = r^2 \lambda^2$ and the 2-dim metric is

$$ds^2 = -\lambda\, r\, \frac{dU'_{D_\pm} dV'_{D_\pm}}{{W_{b'}}^2} \equiv -\frac{dU'_{D_\pm} dV'_{D_\pm}}{(W'_{b'})^2}, \tag{2.13}$$

where $W'_{b'} = \frac{W_{b'}}{\sqrt{\lambda\, r}} = \frac{\alpha_D e^{-T_{b'}}}{\sqrt{\lambda\, r |f(r)|}}$ and $W_{b'}$ is the conformal factor given in (2.12).

Next, we define a new set of Kruskal coordinates for the location of the island boundary (the location of the quantum extremal surface): this turns out be in the black hole interior for the future boundary radiation region, so we require coordinate parametrizations within the black hole horizon. Towards this, we will again first recast the Schwarzschild de Sitter metric (2.1) in the static patch in terms of Kruskal coordinates regular at the black hole horizon. So we define the tortoise coordinate r^* in terms of the parameters β_D, β_S and β_M in the same way as in (2.5), (2.6) and (2.7) in the static patch, in the vicinity of the black hole horizon, with the SdS_4 metric recast as $ds^2 = f(r)(-dt^2 + dr^{*2}) + r^2 d\Omega_2^2$. We label the spacetime coordinates in the left and right regions in the vicinity of the black hole horizon as

$$a_+ : \quad (t,r) = (t_a, a)\,, \qquad a_- : \quad (t,r) = \left(-t_a + \frac{i\beta}{2}, a\right); \qquad \beta = \frac{2\pi}{\alpha_S}\,. \tag{2.14}$$

Here also β takes care of the relative minus signs in the Kruskal coordinates in the left and right regions through $e^{i\beta\alpha_S/2} = e^{i\pi} = -1$. In the static patch around the black hole horizon, the Kruskal coordinates U_S, V_S and the Schwarzschild de Sitter metric become

$$\begin{aligned}
&a_+ : \qquad U_{S_+} = -e^{-\alpha_S(t_a - r^*)}\,, \quad V_{S_+} = e^{\alpha_S(t_a + r^*)},\\
&\alpha_S = \frac{1}{2\beta_S}\,; \quad U_{S_+}V_{S_+} = -e^{2\alpha_S r^*}\,, \qquad \frac{U_{S_+}}{V_{S_+}} = -e^{-2\alpha_S t_a}\,; \quad ds^2 = -\frac{dU_{S_+}dV_{S_+}}{{W_a}^2} + r^2 d\Omega^2\,,\\
&W_a = \sqrt{r}\, l\, \alpha_S (r_D - r)^{-\frac{(1+2\alpha_S\beta_D)}{2}} (r - r_S)^{\frac{(2\alpha_S\beta_S - 1)}{2}} (r + r_S + r_D)^{\frac{(2\alpha_S\beta_M - 1)}{2}}\,.
\end{aligned} \tag{2.15}$$

The value of α_S here ensures regularity at the black hole horizon. (noting $\beta_M + \beta_S = \beta_D$ we see that W has dimensions of inverse length.) With this parametrization of the left and right time coordinates, we use the expressions in (2.15) with β doing the left-right book-keeping.

Towards parametrizing the island boundary inside the black hole horizon, we will analytically continue the spacetime coordinates defined in the static patch near the black hole horizon keeping invariant the metric in terms of the black hole interior Kruskal coordinates. Let us consider the analytic continuation in $(t_a, {r_a}^*)$ coordinates as

$$(t_a, {r_a}^*) \to \left(X_{a'} = \alpha_S\left(t_a - \frac{i\pi}{2\alpha_S}\right), T_{a'} = \alpha_S\left({r_a}^* + \frac{i\pi}{2\alpha_S}\right)\right). \tag{2.16}$$

Thus the new set of Kruskal coordinates at both the island boundaries a'_+ and a'_- are defined as (U'_{S_+}, V'_{S_+}) and (U'_{S_-}, V'_{S_-}) respectively and the Schwarzschild de Sitter metric in terms of $(X_{a'}, T_{a'})$ coordinates becomes

$$\begin{aligned}
&a'_+ : \quad U'_{S_+} = e^{-(X_{a'} - T_{a'})}\,, \qquad V'_{S_+} = e^{(X_{a'} + T_{a'})},\\
&a'_- : \quad U'_{S_-} = e^{(X_{a'} + T_{a'})}\,, \qquad V'_{S_-} = e^{-(X_{a'} - T_{a'})},\\
&\quad U'_{S_\pm}V'_{S_\pm} = e^{2T_{a'}}\,, \qquad \frac{U'_{S_\pm}}{V'_{S_\pm}} = e^{\mp 2X_{a'}}\,; \quad ds^2 = \frac{1}{\alpha_S^2}|f(r)|\left(-dT_{a'}^2 + dX_{a'}^2\right) + r^2 d\Omega^2,\\
&\quad |f(r)| = \frac{1}{l^2 r}(r_D - r)(r_S - r)(r + r_S + r_D)\,.
\end{aligned} \tag{2.17}$$

The Schwarzschild de Sitter metric in terms of Kruskal coordinates becomes

$$\begin{aligned}
&ds^2 = -\frac{dU'_{S_\pm}dV'_{S_\pm}}{{W_{a'}}^2} + r^2 d\Omega^2\,,\\
&W_{a'} = \sqrt{r}\, l\, \alpha_S (r_D - r)^{-\frac{(1+2\alpha_S\beta_D)}{2}} (r_S - r)^{\frac{(2\alpha_S\beta_S - 1)}{2}} (r + r_S + r_D)^{\frac{(2\alpha_S\beta_M - 1)}{2}}\,.
\end{aligned} \tag{2.18}$$

JHEP05(2024)016

Here also after the same dimensional reduction, as in [92], the 2-dim metric beyond the black hole horizon becomes

$$ds^2 = -\lambda\, r \frac{dU'_{S_\pm} dV'_{S_\pm}}{{W_{a'}}^2} \equiv -\frac{dU'_{S_\pm} dV'_{S_\pm}}{(W'_{a'})^2}\,, \tag{2.19}$$

where $W'_{a'} = \frac{W_{a'}}{\sqrt{\lambda r}} = \frac{\alpha_S e^{T_{a'}}}{\sqrt{\lambda r |f(r)|}}$ and $W_{a'}$ is the conformal factor given in (2.18).

3 Entanglement entropy: no island

In this section, we will evaluate the entanglement entropy of the radiation at late times in the absence of any island. Here we have the radiation region R within the interval b'_+ and b'_- as shown in figure 1. We have chosen the bulk matter to be within the above stated interval in some fixed T slice near the future boundary. The entropy of the Hawking radiation is

$$S_{\text{matter}} = S(R)\,. \tag{3.1}$$

We calculate the bulk entropy technically using 2-dimensional techniques where we approximate the bulk matter by a 2-dim CFT propagating in the 2-dim background. In the 2-dim CFT, the matter entanglement entropy for a single interval $A = [x, y]$ is obtained from the replica formulation [142, 143] after also incorporating in $d[x, y]$ the conformal transformation to a curved space [8], stemming from the W'-factor in the 2-dim metric (2.13),

$$S_A = \frac{c}{3} \log d[x, y] = \frac{c}{6} \log\left(\frac{-\Delta U_S \Delta V_S}{W'|_x\, W'|_y}\right). \tag{3.2}$$

So, we obtain the entropy of the bulk matter CFT of the radiation region as

$$S_{\text{matter}} = \frac{c}{3}\, \log\left[d(b'_+, b'_-)\right]. \tag{3.3}$$

Then we evaluate the bulk matter entropy near the future boundary in the Schwarzschild de Sitter geometry (2.13) to obtain (suppressing $1/\epsilon_{\text{UV}}^2$ inside the logarithm, ϵ_{UV} the UV cutoff)

$$S_{\text{matter}} = \frac{c}{6}\, \log\left(\frac{(U'_{D_-} - U'_{D_+})(V'_{D_+} - V'_{D_-})}{W'_{b'_+} W'_{b'_-}}\right). \tag{3.4}$$

Using the Kruskal coordinates (2.11), the bulk matter entanglement entropy then becomes

$$S = \frac{c}{6}\, \log\left[16\lambda \beta_D^2\, (b' - r_D)\, \frac{(b' - r_S)(b' + r_S + r_D)}{l^2}\, \sinh^2(X_{b'})\right]. \tag{3.5}$$

Alongwith ϵ_{UV}^2 and the discussions around (2.13), it can be seen that the logarithm argument is dimensionless (noting from (2.7) that β_D has dimensions of length). The details of the calculation are shown in appendix B. The late time approximation is done by considering large $X_{b'}$, which means we are considering the entire constant T slice: the above result then approximates as

$$S \approx const + \frac{c}{3} X_{b'}\,. \tag{3.6}$$

JHEP05(2024)016

This linear growth of the bulk matter entropy with length $X_{b'}$ means that the entropy of the radiation will eventually be infinitely larger than the Bekenstein-Hawking entropy of the black hole for large $X_{b'}$. This inconsistency is the reflection of the black hole information paradox from the future boundary point of view. See [89] for similar observations in dS_2.

To gain some intuition for this linear growth with "length" at the future boundary relative to linear growth in ordinary time, it is useful to compare the present situation with [92] where we studied the evolution of the entanglement entropy of radiation collected by observers labelled by $b_\pm$ in the left/right static diamond patches (see figure 1) at late times i.e. for large $|t_b|$. In our present context, the future boundary radiation region (b'_+, b'_-) is defined by spacetime coordinates (X'_b, T'_b) obtained by analytic continuation (2.10) of the spacetime coordinates $(t_b, r_b{}^*)$ defined in the static diamond patches. Geometrically, using figure 1, we see that points in the left and right static diamonds can be mapped to points near the future boundary I^+ by drawing out light rays from b_+ to b'_+ and b_- to b'_-. In the late limit with $|t_b|$ large, the points $b_\pm$ in the left/right static diamonds (left/right ends of the blue radiation regions) move towards the top end of the green lines (observer worldlines just inside the cosmological horizon). The corresponding lightrays map this to points near the left/right ends of the future boundary, giving large lengths $|X_{b'}|$, consistent with the analytic continuation (2.10). In other words, the points $b'_\pm$ approach the ends of the future boundary. This is consistent with the picture of Hawking radiation from the black hole eventually crossing the cosmological horizons and reaching the future boundary, so that late times for static patch observers map to large lengths for future boundary (meta)observers. Our future boundary (meta)observers perspective here is reminiscent of the "census-taker" who looks back into the past and collect data [144]: it would be fascinating to make this precise and develop further.

4 Late time entanglement entropy with island

The Hawking radiation from the black hole will eventually cross the cosmological horizon and reach the future boundary (see figure 1), where we imagine it is collected by appropriate (meta)observers. In this section, we will evaluate the entanglement entropy of the bulk matter near the future boundary after including appropriate islands. The island proposal [9] for the fine-grained entropy of the Hawking radiation is

$$S(R) = \min\left\{ \mathrm{ext}\left[\frac{\mathrm{Area}(\partial I)}{4G_N} + S_{\mathrm{matter}}(R\cup I) \right] \right\} \tag{4.1}$$

where R is the region far from the black hole where the radiation is collected by distant observers and I is a spatially disconnected island around the horizon that is entangled with R. The intuition here is that after about half the black hole has evaporated, the outgoing Hawking radiation (roughly I) begins to purify the early radiation (roughly R). This purification by the late Hawking radiation of the early radiation reflects the entanglement between the two parts, stemming from the picture of Hawking radiation as production of entangled particle pairs near the horizon (taken as vacuum). Thus $R\cup I$ purifies over time, its entanglement decreasing. The decreasing area of the slowly evaporating (approximately quasistatic) black hole then leads to $S(R)$ decreasing in time, recovering the falling Page curve expected from unitarity of the original approximately pure state.

JHEP05(2024)016

In the current case, the future boundary receives Hawking radiation from both the left and right black hole horizons so we expect islands on both left and right. Each island almost entirely covers the corresponding black hole interior: the island boundaries are at a'_+ and a'_- (figure 1). The islands in question turn out to emerge just inside the black hole horizon, so

$$b' - r_D \gg r_S - a' \sim 0\,. \tag{4.2}$$

Including an island I at late times i.e. for large $X_{b'}$ and $X_{a'}$, the effective radiation region becomes $\Sigma_{\rm rad} \cup I$. Now we make the assumption that the global vacuum state is approximately pure: this is not strictly true since the bulk matter CFT is expected to be at finite dS temperature in the ambient de Sitter space. However in the limit of a small mass black hole in a very large dS space with correspondingly very low dS temperature, one can take the bulk matter to be at nearly zero temperature and correspondingly in a global pure state. With this assumption, one instead computes the entanglement entropy of the complementary region $(\Sigma_{\rm rad} \cup I)^c$, which comprises the two intervals $[a'_+, b'_+]$ and $[b'_-, a'_-]$, which turns out to be self-consistent.

The entanglement entropy for multiple disjoint intervals

$$A = [x_1, y_1] \ \cup \ [x_2, y_2] \ \cup \ \ldots \ \cup \ [x_N, y_N] \tag{4.3}$$

is more complicated, arising from the multi-point correlation functions of twist operators: so it depends on not just the central charge but detailed CFT information. In the limit where the intervals are well-separated, expanding the twist operator products yields [142, 143, 145, 146]

$$S_A = \frac{c}{3} \log \frac{\prod_{i,j} d[x_j, y_i]}{\prod_{i<j} d[x_j, x_i] \ \ \prod_{i<j} d[y_j, y_i]} \tag{4.4}$$

For two intervals $[x_1, y_1] \cup [x_2, y_2]$, this is a limit where the cross ratio x is small, i.e. $x \ll 1$, with $x = \frac{d[x_1,y_1]\, d[x_2,y_2]}{d[x_1,x_2]\, d[y_1,y_2]}$, and we use the Kruskal distances in (3.2) in constructing the cross-ratio. In 2-dim CFTs with a holographic dual, this is the situation where the two intervals A, B are well-separated and their mutual information exhibits a disentangling transition [147] with $I[A, B] = S[A] + S[B] - S[A \cup B] \to 0$, i.e. the disconnected surface $S_{\rm dis} = S[A] + S[B]$ has lower area than the connected surface $S_{\rm conn} = S[A \cup B]$. Assuming an approximate global pure state, we are considering the complementary region as the 2-interval region $(\Sigma_{\rm rad} \cup I)^c = [a'_+, b'_+] \cup [b'_-, a'_-]$. When the future boundary interval $[b'_+, b'_-]$ is large approaching the entire future boundary, the two intervals are well-separated (as seen from figure 1), so the cross-ratio above is indeed small, justifying the use of (4.4) for our purposes (we have $1 - x = \frac{d[a'_+,a'_-]\, d[b'_+,b'_-]}{d[a'_+,b'_-]\, d[a'_-,b'_+]} \sim 1$ here). In this limit of approaching the entire future boundary, we have large $b'_\pm$, amounting to the assumption (4.2) here. Note that there is no holography here: we are simply applying the island rule in the 2-dim background obtained from reduction of the SdS_4 geometry and looking for self-consistent island configurations, assuming an approximate global pure state in the very low de Sitter temperature limit. It is also worth noting that while the complementary 2-interval region is unambiguously defined, the 3-interval region is more ambiguous. For instance, in figure 1, one might imagine defining a global Cauchy slice as the spacelike slice passing through the points

$\{\frac{(a'_-+a'_+)_L}{2},\ a'_+,\ b'_+,\ b'_-,\ a'_-,\ \frac{(a'_-+a'_+)_R}{2}\}$, where the left/right endpoints are the approximate midpoints of the left/right islands (and this "unit cell" repeats indefinitely along the Penrose diagram). Then the 2-interval subregion $(\Sigma_{\rm rad}\cup I)^c = [a'_+, b'_+]\cup[b'_-, a'_-]$ is complementary to the 3-interval subregion $\Sigma_{\rm rad}\cup I = [\frac{(a'_-+a'_+)_L}{2},\ a'_+]\cup[b'_+, b'_-]\cup[a'_-,\ \frac{(a'_-+a'_+)_R}{2}]$ on this Cauchy slice. It would appear that there is nothing sacrosanct in choosing these midpoints $\frac{(a'_-+a'_+)_{L,R}}{2}$ to define the slice, whereas the 2-interval complement is well-defined via the radiation region and island endpoints. It would be interesting to understand this more elaborately.

In light of the above, the entanglement entropy for the complementary 2-interval region $[a'_+, b'_+]\cup[b'_-, a'_-]$ using (4.4) is

$$S_{\rm matter} = \frac{c}{3}\log\frac{d[a'_+, a'_-]\,d[b'_+, b'_-]\,d[a'_+, b'_+]\,d[a'_-, b'_-]}{d[a'_+, b'_-]\,d[a'_-, b'_+]}\,. \tag{4.5}$$

In detail, using the Kruskal coordinates (2.11), (2.17), the total generalized entropy (4.5) becomes

$$\begin{aligned} S_{\rm total} = \frac{2\pi a'^2}{G_N} &+ \frac{c}{6}\log\Bigg[\frac{2^4\lambda^2}{\alpha_D^2\alpha_S^2}(r_S-a')(b'-r_S)\left(\frac{r_D-a'}{l}\right)\left(\frac{b'-r_D}{l}\right)\cdot \\ &\qquad\qquad \left(\frac{a'+r_S+r_D}{l}\right)\left(\frac{b'+r_S+r_D}{l}\right)\sinh^2 X_{a'}\sinh^2 X_{b'}\Bigg] \\ &+\frac{c}{3}\log\left[1-2\frac{(r_S-a')^{\alpha_S\beta_S}}{(b'-r_D)^{\alpha_D\beta_D}}\,C(a')\,\cosh\left(X_{a'}+X_{b'}\right)\right] \\ &-\frac{c}{3}\log\left[1-2\frac{(r_S-a')^{\alpha_S\beta_S}}{(b'-r_D)^{\alpha_D\beta_D}}\,C(a')\,\cosh\left(X_{a'}-X_{b'}\right)\right], \end{aligned} \tag{4.6}$$

where we have added the area term, and $C(a')$ is defined as

$$C(a') = \frac{(b'-r_s)^{\alpha_D\beta_S}(a'+r_S+r_D)^{\alpha_S\beta_M}(b'+r_S+r_D)^{\alpha_D\beta_M}}{(r_D-a')^{\alpha_S\beta_D}}\,. \tag{4.7}$$

(Note from (2.7) that $C(a')$ is dimensionless.) See appendix C for details of this calculation.

Extremizing (4.6) with respect to the location of the island boundary a' as $\frac{\partial S_{\rm total}}{\partial a'}=0$ gives

$$\begin{aligned} &\frac{4\pi a'}{G_N}+\frac{c}{6}\left[-\frac{1}{r_S-a'}-\frac{1}{r_D-a'}+\frac{1}{a'+r_S+r_D}\right] \\ &-\frac{c}{3}\frac{C(a')}{\sqrt{b'-r_D}\sqrt{r_S-a'}}\left[-1+2(r_S-a')\left(\frac{\alpha_S\beta_M}{a'+r_S+r_D}+\frac{\alpha_S\beta_D}{r_D-a'}\right)\right]\cdot \\ &\qquad\Bigg[\frac{\cosh(X_{a'}+X_{b'})}{1-2\frac{(r_S-a')^{\alpha_S\beta_S}}{(b'-r_D)^{\alpha_D\beta_D}}\,C(a')\,\cosh\left(X_{a'}+X_{b'}\right)} \\ &\qquad\quad -\frac{\cosh(X_{a'}-X_{b'})}{1-2\frac{(r_S-a')^{\alpha_S\beta_S}}{(b'-r_D)^{\alpha_D\beta_D}}\,C(a')\,\cosh\left(X_{a'}-X_{b'}\right)}\Bigg]=0\,. \end{aligned} \tag{4.8}$$

Here, since r_D is large, the terms scaling as $O(\frac{1}{r_D})$ can be ignored: thus the $\frac{1}{a'+r_S+r_D}$ and $\frac{1}{r_D-a'}$ are suppressed relative to $\frac{1}{r_S-a'}$. With these approximations, (4.8) becomes

$$\begin{aligned}\frac{4\pi a'}{G_N}-\frac{c}{6}\frac{1}{r_S-a'}+\frac{c}{3}\frac{C(a')}{\sqrt{b'-r_D}\sqrt{r_S-a'}}\cdot\Bigg[&\frac{\cosh(X_{a'}+X_{b'})}{1-2\frac{(r_S-a')^{\alpha_S\beta_S}}{(b'-r_D)^{\alpha_D\beta_D}}C(a')\cosh\left(X_{a'}+X_{b'}\right)}\\&-\frac{\cosh(X_{a'}-X_{b'})}{1-2\frac{(r_S-a')^{\alpha_S\beta_S}}{(b'-r_D)^{\alpha_D\beta_D}}C(a')\cosh\left(X_{a'}-X_{b'}\right)}\Bigg]=0\,.\end{aligned}\tag{4.9}$$

Next, extremizing (4.6) with respect to $X_{a'}$ as $\frac{\partial S_{\text{total}}}{\partial X_{a'}}=0$ gives

$$\begin{aligned}\coth X_{a'}=2\sqrt{\frac{r_S-a'}{b'-r_D}}C(a')\cdot\Bigg[&\frac{\sinh(X_{a'}+X_{b'})}{1-2\frac{(r_S-a')^{\alpha_S\beta_S}}{(b'-r_D)^{\alpha_D\beta_D}}C(a')\cosh\left(X_{a'}+X_{b'}\right)}\\&-\frac{\sinh(X_{a'}-X_{b'})}{1-2\frac{(r_S-a')^{\alpha_S\beta_S}}{(b'-r_D)^{\alpha_D\beta_D}}C(a')\cosh\left(X_{a'}-X_{b'}\right)}\Bigg]\end{aligned}\tag{4.10}$$

We will consider all possible conditions between $X_{a'}$ and $X_{b'}$ in the extremization equations to look for consistent solutions to the location of island boundary, i.e. the value of a' and $X_{a'}$.

We will first consider, $X_{a'}=X_{b'}\Rightarrow X_{a'}-X_{b'}=0$ and $X_{a'}+X_{b'}=2X_{a'}$ for large $X_{a'}$ and $X_{b'}$. Then (4.10) becomes

$$1-2\sqrt{\frac{r_S-a'}{b'-r_D}}C(a')\cosh 2X_{a'}=2\sqrt{\frac{r_S-a'}{b'-r_D}}C(a')\frac{\sinh 2X_{a'}}{\coth X_{a'}}\tag{4.11}$$

Putting this condition (4.11) back in (4.9) gives

$$\begin{aligned}&\frac{4\pi a'}{G_N}-\frac{c}{6}\frac{1}{r_S-a'}+\frac{c}{3}\frac{C(a')}{\sqrt{b'-r_D}\sqrt{r_S-a'}}\left[\frac{\cosh(2X_{a'})}{2\frac{(r_S-a')^{\alpha_S\beta_S}}{(b'-r_D)^{\alpha_D\beta_D}}C(a')\frac{\sinh 2X_{a'}}{\coth X_{a'}}}-1\right]=0\\ \Rightarrow\;&\frac{4\pi a'}{G_N}-\frac{c}{3}\frac{C(a')}{\sqrt{b'-r_D}\sqrt{r_S-a'}}-\frac{c}{6}\frac{1}{r_S-a'}\left(1-\frac{\coth X_{a'}}{\tanh 2X_{a'}}\right)=0\,.\end{aligned}\tag{4.12}$$

For large $X_{a'}$ and $X_{b'}$, the third term in (4.12) is small compared to the second term. So we can ignore the third term and (4.12) becomes

$$a'\simeq\frac{1}{\sqrt{r_S-a'}}\frac{G_N c}{12\pi}\frac{1}{\sqrt{b'-r_D}}C(a')\,.\tag{4.13}$$

Now we recall that we are in the semiclassical regime where

$$0\ll c\ll\frac{1}{G_N}\,,\tag{4.14}$$

so that the classical area term in the generalized entropy is dominant but the bulk matter makes nontrivial subleading contributions (which are not so large as to cause significant backreaction on the classical geometry).

We are looking for an island with boundary $a'\sim r_S$ near the black hole horizon: this corroborates with the fact that since the entire right hand side in (4.13) is $O(G_N c)$, in the classical limit $G_N c = 0$ we obtain $a'\sqrt{r_s - a'} \simeq O(G_N c) \sim 0$ giving $a' = r_S$, i.e. the quantum extremal surface localizes on the black hole horizon. Thus we can solve the above extremization equation in perturbation theory setting $a' \sim r_S$ at leading order to find the first order correction in $G_N c \ll 1$: then schematically we have

$$r_S - a' \simeq \frac{K^2}{r_S^2}\frac{1}{b' - r_D}\,, \qquad K = \frac{G_N c}{12\pi}C(r_S)\,. \tag{4.15}$$

Thus, we finally obtain (with $C(r_S)$ from (4.7) setting $a' = r_S$)

$$a' \simeq r_S - \frac{(G_N c)^2}{144\pi^2 r_S^2 (b' - r_D)}C(r_S)^2. \tag{4.16}$$

Solving now for $X_{a'}$ from (4.10), we obtain

$$\cosh 2X_{a'} = \frac{6\pi}{G_N c}\frac{r_S(b' - r_D)}{C(r_S)^2}\frac{\coth X_{a'}}{\tanh 2X_{a'} + \coth X_{a'}}\,. \tag{4.17}$$

This is a large $X_{a'}$ value with $e^{2X_{a'}}$ scaling approximately as $O(\frac{1}{G_N c})$. Considering $X_{a'} \sim -X_{b'}$ does not yield consistent island solutions: see appendix D.2. Further, considering potential island solutions just outside the horizon turns out to be inconsistent: see appendix D.1. Thus (4.16), (4.17), with $X_{a'} \sim X_{b'}$, encode the correct island solution for the future boundary radiation region. The condition $X_{a'} = X_{b'}$ is consistent with the expectation that the island location lies on the same Cauchy slice as the radiation region location (along the same lines as the condition $t_a = t_b$ within the static diamond in [92])). This amounts to the requirement of spacelike separation in considering the island and radiation as an effectively single entity which purifies so the fact that we recover this is not surprising. The fact that islands outside the horizon are inconsistent is due to causality: the entanglement wedge cannot lie within the causal wedge (we explain this further in the Discussion section 5).

With the value of a' in (4.16) and $X_{a'}$ in (4.17), the total on-shell entanglement entropy in (4.6) becomes

$$\begin{aligned} S_{o.s} = {} & \frac{2\pi r_S^2}{G_N} - \frac{c^2 G_N}{36\pi r_S(b'-r_D)}C(r_S)^2 \\ & + \frac{c}{6}\log\left[\frac{16\lambda^2\beta_s^2\beta_D^2(b'-r_D)^2}{l^4}\frac{(r_D-r_S)^{1+2\alpha_S\beta_D}}{(b'-r_S)^{2\alpha_S\beta_D-1}(2r_S+r_D)^{2\alpha_S\beta_M-1}(b'+r_S+r_D)^{2\alpha_S\beta_M-1}}\right]. \end{aligned} \tag{4.18}$$

which is independent of length $X_{a'}$ and $X_{b'}$, stemming from the presence of the island. The leading first (area) term is twice the Bekenstein-Hawking entropy of the black hole, while the subleading second and third terms arising from the bulk entropy of the radiation region purified by the island are constant terms not growing in length. This recovers the expectations on the Page curve for the entropy of the bulk matter or Hawking radiation considered near the future boundary. The bulk matter at the future boundary radiation region is entangled with the island-like region located just inside the black hole interior in these semiclassical approximations at very low ambient de Sitter temperature.

Comparing the entanglement entropy without the island (3.6) and that with the island (4.18) provides the critical length X_{Page} at which the island transition occurs: we obtain

$$\frac{c}{3}X_{\text{Page}} \sim 2S_{\text{BH}} \quad \Rightarrow \quad X_{\text{Page}} \sim \frac{6\pi {r_S}^2}{G_N c}\,. \tag{4.19}$$

The entropy with the island alongwith the associated purification is lower and dominates over the no-island configuration beyond this critical length X_{Page}. Note that here the critical Page length X_{Page} is a dimensionless quantity, using (2.10). This then corresponds to a Page time $t_P \sim \beta_D X_{\text{Page}}$ which using (2.7) and the approximations (2.3) gives the large value $t_P \sim l S_{\text{BH}}$ (note that this uses the cosmological Kruskal coordinates, distinct from the black hole Kruskal coordinates in [92]). It is however important to note that this Page length is much smaller than another potentially relevant quantity $X_P^{\text{dS}} \sim S_{\text{dS}}$ controlled by the entropy S_{dS} of the cosmological horizon. In the small black hole limit (2.3) we are considering, $S_{\text{dS}} \sim \frac{l^2}{G_N} \gg S_{\text{BH}} \sim \frac{r_S^2}{G_N}$, and we do not see any effects above, stemming from the ambient de Sitter space which is just a frozen background. So our critical Page length (4.19) controlled by black hole entropy alone is consistent with the separation of scales in the limit (2.3). Away from this limit, the black hole horizon shrinks while the cosmological horizon absorbs and grows, resulting in a nontrivial nonequilibrium system. It would of course be interesting to understand de Sitter horizon physics, but this appears substantially more challenging within our framework.

Finally, it is worth noting that there are also timelike separated quantum extremal surface solutions following from the extremization of the generalized entropy with respect to the future boundary observer: we discuss these solutions in appendix E. The timelike separation implies that the on-shell generalized entropy becomes complex valued. While complex entropies are known in investigations in pure de Sitter space (which does not have a sufficiently wide Penrose diagram) and suggest new objects [123–127], it is consistent to ignore them in the Schwarzschild de Sitter context where spacelike separated quantum extremal surfaces do exist in accord with physical Page curve expectations for the black hole information paradox.

5 Discussion

We have studied small 4-dim Schwarzschild de Sitter black holes in the limit of very low de Sitter temperature, building further on previous work [92] for observers within the static diamond far from the black hole horizon. In the present work, we have been considering the black hole Hawking radiation in a radiation region interval at the future boundary (see figure 1). The black hole mass is adequately large that quasistatic approximations to the evaporating black hole in semiclassical gravity are valid. We assume the black hole radiation approximated as a 2-dim CFT at nearly zero temperature propagating in a 2-dim dilaton gravity background (2.13) obtained by dimensional reduction of the 4-dim spacetime. Including appropriate island contributions, we find that the generalized entropy satisfies expectations from the Page curve for the evolution of bulk matter near the future boundary. Our analysis has parallels with [89] which studied island resolutions for dS_2 JT gravity with regard to the future boundary. Our setup here is somewhat more complicated since the assumption of an approximate global pure state is only reasonable, if at all, at very low de Sitter temperature. The fact that these approximate calculations vindicate the island paradigm perhaps suggests the existence of better, more fundamental ways to formulate the information paradox in such nontrivial gravitational backgrounds and of deeper insights into replica wormholes in these sorts of quasistatic gravitational backgrounds.

JHEP05(2024)016

The Schwarzschild de Sitter (SdS) black hole is unstable and thus somewhat different from the AdS black hole. In our small black hole limit (2.3) the ambient de Sitter space effectively remains a frozen background reservoir. In a quasistatic approximation, the black hole evaporates away slowly, and our analysis using the eternal SdS black hole shows the radiation entanglement entropy including the island becoming saturated at some finite value (4.18), approximately $2S_{\rm BH}$ (so the Page curve saturates rather than falls). As the black hole evaporates, its entropy decreases so the saturation value of the radiation entropy decreases leading to the black hole Page curve falling slowly in accord with the approximately pure state that the black hole formed from. Strictly speaking, the ambient de Sitter space temperature (albeit much lower than that of the black hole) implies that the pure state consideration is just an approximation. It would be interesting to study the SdS black hole modelling the bulk matter CFT in the thermal state at finite de Sitter temperature.

We recall that in [92], the radiation region was within the static diamond (with endpoints b_+ or b_- in the left or right static diamond, in figure 1). The late time island location was then found to be within the static diamond, just outside the black hole horizon in that case. As we have seen, the island location we have found currently is just inside the black hole horizon, which at first sight might seem contradictory. However this is in fact consistent in the current case. First, the future boundary interval (b'_+, b'_-) in the present case receives Hawking radiation from both the left and right black hole patches, propagating past the left and right cosmological horizons bounding the left and right static diamonds. So this setup is physically distinct from the previous case of a single static diamond. Secondly, in obtaining the island locations we have been considering the limit of large $X_{a'}, X_{b'}$, in the extremization equations. In this limit the future boundary interval (b'_+, b'_-) approaches the entire future boundary, i.e. the points $b'_\pm$ approach the endpoints of I^+. Note that the left and right static diamonds are now within the causal wedge of this interval. It would then be causally inconsistent for the entanglement wedge to be within the causal wedge of the radiation interval. The entanglement wedge of the radiation region is the domain of dependence, or bulk causal diamond of the spacelike surface between the boundary of the radiation region and the island boundary (location of quantum extremal surface). As it stands, the island boundary is just inside the black hole horizon so it lies outside the causal wedge, nicely avoiding inconsistency.

The black hole interior island solution is ultimately supported by the calculational fact that other possibilities lead to inconsistencies: for instance, blindly looking for island solutions outside the horizon in the present case exhibits inconsistency in the extremization equations. We carried out this exercise by performing the calculation of section 4 using static diamond Kruskal coordinates for the potential island lying just outside the black hole horizon in the static diamond ($a' \gtrsim r_s$ in this case, somewhat akin to the parametrizations in [92] reviewed in appendix A). The analog of (4.6) in this case leads to extremization equations similar to (4.8) and (4.10): however there are subtle differences which ensure that the analogs of (4.11) and (4.12) together do not give consistent island solutions (see appendix D.1). Further, as we also noted after (4.17), potential island solutions with $X_{a'} = -X_{b'}$ (instead of $X_{a'} = X_{b'}$) also lead to inconsistencies (appendix D.2). Thus overall, our semiclassical island solution in (4.16) and (4.17) should be regarded as nontrivial. Perhaps the self-consistency of these calculations (in particular using the complementary 2-interval bulk matter entropy) also

JHEP05(2024)016

vindicates the assumption of approximate purity of the initial matter that made the black hole in this very low temperature de Sitter ambience. It would be interesting to explore this in more detail, as discussed around (4.4).

The separation of scales in the small black hole limit (2.3) ensures that black holes can be regarded as localized subsystems analyzable by distinct classes of observers (or metaobservers). Then, abstracting away from our technical analysis in Schwarzschild de Sitter black holes vindicates some general lessons for the black hole information paradox here as well. Islands appear to emerge self-consistently evading paradoxes with (i) unitarity as encapsulated by the Page curve (late static patch times and large future boundary lengths), (ii) causality (the island boundary does not lie within the causal wedge), (iii) overcounting (the purifying island is spacelike separated from the radiation, lying on the same Cauchy slice). In this light, de Sitter space itself and cosmological horizons appear exotic: extremal surfaces anchored at the future boundary involve timelike separations (e.g. [68, 86], for quantum extremal surfaces, and [123–127] for classical RT/HRT surfaces). So de Sitter space, and perhaps cosmology more generally, require new insights.

Our discussions of Schwarzschild de Sitter are entirely within the bulk framework of semiclassical gravity, with no holography per se (except in the broad sense of gravity being intrinsically holographic). The future boundary is well-defined as a place where gravity is manifestly weak: however we have simply applied the island formulation in these relatively complicated higher dimensional models under various assumptions and approximations without rigorous justification. So this appears to stretch the regimes of validity of the original island proposals, although it corroborates the general expectations laid out in [18]. It would be nice to better understand in more fundamental ways the deeper underpinnings of semiclassical gravity that encode these self-consistent island formulations of the black hole information paradox. In this regard it might be interesting to understand the interplay between the generalized entropy and its extremization and gravity actions (see e.g. [89, 148–150]) in the context of the general 2-dim dilaton gravity theories (2.13) we consider here arising from reduction of SdS_4.

Acknowledgments

It is a pleasure to thank Ahmed Almheiri, Sitender Kashyap, Alok Laddha, Juan Maldacena, Suvrat Raju and Amitabh Virmani for discussions and comments on a draft. This work is partially supported by a grant to CMI from the Infosys Foundation.

A Review: static patch radiation entropy with islands

In this section, we briefly review the calculation in [92] of the island resolution of the black hole information paradox in Schwarzschild de Sitter black holes in the limit of small black hole mass and very low de Sitter temperature. This has close parallels with islands in flat space Schwarzschild black holes [26]. Considering the radiation region in the static patch, far from the black hole horizon but within the cosmological horizon, the entanglement entropy of the bulk matter can be shown to increase unboundedly. Including an island region $I \equiv [a_-, a_+]$ straddling across the black hole horizon, we consider the entanglement entropy

JHEP05(2024)016

of the interval $R_- \cup I \cup R_+$. Strictly speaking, the bulk matter should be approximated as a CFT at finite temperature corresponding to the de Sitter temperature: however in the limit of very low de Sitter temperature and a small mass black hole, we can approximate the bulk theory to be in an approximately pure state. Then calculating the complementary interval entropy and appending the area term (from the island boundary area) gives the total entanglement entropy [92]

$$\begin{aligned}S_{\text{total}} = \frac{2\pi a^2}{G_N} + \frac{c}{6}\log\Bigg[&\frac{2^8 r_S^4}{(\frac{r_D - r_S}{l})^4(\frac{2r_S + r_D}{l})^4}(a-r_S)(b-r_S)\left(\frac{a-r_D}{l}\right)\left(\frac{b-r_D}{l}\right)\cdot \\ &\left(\frac{a+r_S+r_D}{l}\right)\left(\frac{b+r_S+r_D}{l}\right)\cosh^2\frac{t_a}{2\beta_S}\cosh^2\frac{t_b}{2\beta_S}\Bigg] \\ &+\frac{c}{3}\log\left[1 - 2\frac{(a-r_S)^{\alpha_S\beta_S}}{(b-r_S)^{\alpha_S\beta_S}}C(a)\,\cosh\left(\alpha_S(t_a-t_b)\right)\right] \\ &-\frac{c}{3}\log\left[1 + 2\frac{(a-r_S)^{\alpha_S\beta_S}}{(b-r_S)^{\alpha_S\beta_S}}C(a)\,\cosh\left(\alpha_S(t_a+t_b)\right)\right],\end{aligned} \tag{A.1}$$

where $C(a)$ is

$$C(a) = \frac{(r_D - b)^{\alpha_S\beta_D}(a + r_S + r_D)^{\alpha_S\beta_M}}{(r_D - a)^{\alpha_S\beta_D}(b + r_S + r_D)^{\alpha_S\beta_M}}. \tag{A.2}$$

Extremizing S_{total} in (A.1) with respect to the location of the island boundary a gives

$$\begin{aligned}\frac{4\pi a}{G_N} + \frac{c}{6}\frac{1}{a-r_S} - \frac{c}{3}\frac{C(a)}{\sqrt{b-r_S}\sqrt{a-r_S}}\Bigg[&\frac{\cosh(\alpha_S(t_a-t_b))}{1-2\frac{(a-r_S)^{\alpha_S\beta_S}}{(b-r_S)^{\alpha_S\beta_S}}C(a)\,\cosh\left(\alpha_S(t_a-t_b)\right)} \\ &+\frac{\cosh\left(\alpha_S(t_a+t_b)\right))}{1+2\frac{(a-r_S)^{\alpha_S\beta_S}}{(b-r_S)^{\alpha_S\beta_S}}C(a)\,\cosh\left(\alpha_S(t_a+t_b)\right)}\Bigg] = 0\,.\end{aligned} \tag{A.3}$$

Next, extremizing S_{total} from (A.1) with respect to t_a gives

$$\begin{aligned}\tanh\left(\alpha_S t_a\right) = 2\sqrt{\frac{a-r_S}{b-r_S}}C(a)\alpha_S\Bigg[&\frac{\sinh(\alpha_S(t_a-t_b))}{1-2\frac{(a-r_S)^{\alpha_S\beta_S}}{(b-r_S)^{\alpha_S\beta_S}}C(a)\,\cosh\left(\alpha_S(t_a-t_b)\right)} \\ &+\frac{\sinh(\alpha_S(t_a+t_b))}{1+2\frac{(a-r_S)^{\alpha_S\beta_S}}{(b-r_S)^{\alpha_S\beta_S}}C(a)\,\cosh\left(\alpha_S(t_a+t_b)\right)}\Bigg]\end{aligned} \tag{A.4}$$

First consider $t_a = t_b$ so $t_a - t_b = 0$ and $t_a + t_b = 2t_a$ for large t_a, t_b. Then (A.4) becomes

$$1 + 2\sqrt{\frac{a-r_S}{b-r_S}}C(a)\cosh\left(\alpha_S\cdot 2t_b\right) = 2\sqrt{\frac{a-r_S}{b-r_S}}C(a)\frac{\sinh\left(\alpha_S\cdot 2t_b\right)}{\tanh\left(\alpha_S t_b\right)} \tag{A.5}$$

Next, putting this condition (A.5) back in (A.3) gives

$$\begin{aligned}&\frac{4\pi a}{G_N} + \frac{c}{6}\frac{1}{a-r_S} - \frac{c}{3}\frac{C(a)}{\sqrt{b-r_S}\sqrt{a-r_S}}\left[1+\frac{\cosh\left(\alpha_S\cdot 2t_b\right)}{2\frac{(a-r_S)^{\alpha_S\beta_S}}{(b-r_S)^{\alpha_S\beta_S}}C(a)\,\frac{\sinh\left(\alpha_S\cdot 2t_b\right)}{\tanh\left(\alpha_S t_b\right)}}\right] = 0 \\ &\Rightarrow \frac{4\pi a}{G_N} - \frac{c}{3}\frac{C(a)}{\sqrt{b-r_S}\sqrt{a-r_S}} + \frac{c}{6}\frac{1}{a-r_S}\left(1 - \frac{\tanh\left(\alpha_S t_b\right)}{\tanh\left(\alpha_S\cdot 2t_b\right)}\right) = 0\,.\end{aligned} \tag{A.6}$$

For large t_a and t_b, the third term in (A.6) is small relative to the second term. So we can ignore the third term and (A.6) becomes

$$a \simeq \frac{1}{\sqrt{a-r_S}} \frac{G_N c}{12\pi} \frac{1}{\sqrt{b-r_S}} C(a)\,. \tag{A.7}$$

Thus solving this in perturbation theory for the first order correction in $G_N c \ll 1$ gives

$$a \simeq r_S + \frac{(G_N c)^2}{144\pi^2 r_S^2 (b-r_S)} C(r_S)^2\,, \tag{A.8}$$

setting $a \sim r_S$ in $C(a)$ etc. Solving for t_a from (A.4), we obtain

$$\cosh\left(\alpha_S \cdot 2t_a\right) = \frac{6\pi}{G_N c} \frac{r_S(b-r_S)}{C(r_S)^2} \frac{\tanh\left(\alpha_S t_a\right)}{\tanh\left(\alpha_S \cdot 2t_a\right) - \tanh\left(\alpha_S t_b\right)} \tag{A.9}$$

Equations (A.8), (A.9), at late times $t_a = t_b$, recover the result in [92]. (Considering $t_a = -t_b$ i.e. $t_a + t_b = 0$ and $t_a - t_b = 2t_a$ for large t_a and t_b, the above analysis can be seen to give physically inconsistent solutions.) The island is a little outside the horizon. The late time generalized entropy including the island contribution is finite, approximately twice the black hole entropy upto small corrections from the bulk matter.

B Details: entropy in the no-island case

This section contains some details on the calculations of entanglement entropy in the absence of the island in section 3. Using (2.11) and calculating each part of S_{matter} in (3.4) separately gives

$$U'_{D_-} - U'_{D_+} = -e^{-T_{b'}} \cdot 2\sinh X_{b'}\,, \qquad V'_{D_+} - V'_{D_-} = -e^{-T_{b'}} \cdot 2\sinh X_{b'}\,, \tag{B.1}$$

$$W_{b'_+} = W_{b'_-} = \sqrt{b'}\, l\, \alpha_D\, (b'-r_D)^{-\frac{1-2\alpha_D\beta_D}{2}} (b'-r_S)^{-\frac{1+2\alpha_D\beta_S}{2}} (b'+r_S+r_D)^{-\frac{1+2\alpha_D\beta_M}{2}}\,, \tag{B.2}$$

$$\begin{aligned} W_{b'_+} W_{b'_-} &= b'\, l^2\, \alpha_D^2 (b'-r_D)^{-(1-2\alpha_D\beta_D)} (b'+r_S+r_D)^{-(1+2\alpha_D\beta_M)} (b'-r_S)^{-(1+2\alpha_D\beta_S)} \\ &= \frac{\alpha_D^2}{\lambda b' |f(b')|} e^{-2T_{b'}}\,. \end{aligned} \tag{B.3}$$

Plugging all these into (3.4) gives $S_{\text{matter}} = \frac{c}{6} \log[\frac{\lambda b'}{\alpha_D^2} e^{2T_{b'}} |f(b')| e^{-2T_{b'}} 4\sinh^2 X_{b'}]$, i.e.

$$S_{\text{matter}} = \frac{c}{6} \log\left[\frac{\lambda}{l^2 \alpha_D^2} (b'-r_S)\,(b'-r_D)(b'+r_S+r_D)\, 4\sinh^2 X_{b'}\right]. \tag{B.4}$$

Thus finally, we obtain (3.5).

C Details: late-time entropy with island

Here we give details on section 4. We are looking to calculate (4.5), i.e.

$$S_{\text{matter}} = \frac{c}{3} \log \frac{d(a'_+, a'_-) d(b'_+, b'_-) d(a'_+, b'_+) d(a'_-, b'_-)}{d(a'_+, b'_-) d(a'_-, b'_+)}\,. \tag{C.1}$$

Now calculating each part in S_{matter} separately

$$\log[d(a'_+,a'_-)] = \frac{1}{2}\log\frac{[(U'_{S_-}-U'_{S_+})(V'_{S_+}-V'_{S_-})]}{W'_{a'_+}W'_{a'_-}} \tag{C.2}$$

with $W_{a'}$ as in (2.18). Then we have

$$U'_{S_-}-U'_{S_+} = e^{T_{a'}}\cdot 2\sinh X_{a'}\,, \qquad V'_{S_+}-V'_{S_-} = e^{T_{a'}}\cdot 2\sinh X_{a'}\,, \tag{C.3}$$

$$\begin{aligned} W_{a'_+}W_{a'_-} &= a'l^2\alpha_S^2(r_D-a')^{-(1+2\alpha_S\beta_D)}(a'+r_S+r_D)^{(2\alpha_S\beta_M-1)}(r_S-a')^{(2\alpha_S\beta_S-1)} \\ &= \frac{\alpha_S^2}{\lambda a'|f(a')|}e^{2T_{a'}}\,. \end{aligned} \tag{C.4}$$

Putting all these expressions together in (C.2) gives

$$\begin{aligned} \log[d(a'_+,a'_-)] &= \frac{1}{2}\log\left[\frac{\lambda a'}{\alpha_S^2}e^{-2T_{a'}}|f(a')|e^{2T_{a'}}4\sinh^2 X_{a'}\right] \\ &= \frac{1}{2}\log\left[\frac{\lambda}{l^2\alpha_S^2}(r_D-a')(r_S-a')(a'+r_S+r_D)\cdot 4\sinh^2 X_{a'}\right]. \end{aligned} \tag{C.5}$$

Similarly we obtain

$$\log[d(b'_+,b'_-)] = \frac{1}{2}\log\left[\frac{\lambda}{l^2\alpha_D^2}(b'-r_D)(b'-r_S)(b'+r_S+r_D)\cdot 4\sinh^2 X_{b'}\right]. \tag{C.6}$$

Now, putting (C.5) and (C.6) together gives

$$\begin{aligned} \frac{c}{3}\log[d(a'_+,a'_-)d(b'_+,b'_-)] = \frac{c}{6}\log&\left[\frac{2^4\lambda^2}{\alpha_D^2\alpha_S^2}(r_S-a')(b'-r_S)\left(\frac{r_D-a'}{l}\right)\left(\frac{b'-r_D}{l}\right)\right. \\ &\left.\cdot\left(\frac{a'+r_S+r_D}{l}\right)\left(\frac{b'+r_S+r_D}{l}\right)\sinh^2 X_{a'}\sinh^2 X_{b'}\right]. \end{aligned} \tag{C.7}$$

We next calculate other relevant contributions using (2.11) and (2.17): we have

$$\begin{aligned} U'_{D_+}-U'_{S_+} &= e^{(X_{b'}-T_{b'})}-e^{-(X_{a'}-T_{a'})}, \qquad & V'_{S_+}-V'_{D_+} &= e^{(X_{a'}+T_{a'})}-e^{-(X_{b'}+T_{b'})}\,, \\ U'_{D_-}-U'_{S_-} &= e^{-(X_{b'}+T_{b'})}-e^{(X_{a'}+T_{a'})}, \qquad & V'_{S_-}-V'_{D_-} &= e^{-(X_{a'}-T_{a'})}-e^{(X_{b'}-T_{b'})}\,, \end{aligned}$$

so

$$\begin{aligned} d(a'_+,b'_+) &= \frac{1}{\sqrt{W'_{a'_+}W'_{b'_+}}}\Big[(U'_{D_+}-U'_{S_+})(V'_{S_+}-V'_{D_+})\Big]^{\frac{1}{2}} \\ &= \frac{1}{\sqrt{W'_{a'_+}W'_{b'_+}}}\left[e^{(T_{a'}-T_{b'})}\cdot\Big(2\cosh\left(X_{a'}+X_{b'}\right)-2\cosh\left(T_{a'}+T_{b'}\right)\Big)\right]^{\frac{1}{2}}, \end{aligned} \tag{C.8}$$

$$\begin{aligned} d(a'_-,b'_-) &= \frac{1}{\sqrt{W'_{a'_-}W'_{b'_-}}}\Big[(U'_{D_-}-U'_{S_-})(V'_{S_-}-V'_{D_-})\Big]^{\frac{1}{2}} \\ &= \frac{1}{\sqrt{W'_{a'_-}W'_{b'_-}}}\left[e^{(T_{a'}-T_{b'})}\cdot\Big(2\cosh\left(X_{a'}+X_{b'}\right)-2\cosh\left(T_{a'}+T_{b'}\right)\Big)\right]^{\frac{1}{2}}. \end{aligned} \tag{C.9}$$

JHEP05(2024)016

Now, putting (C.8) and (C.9) together

$$d(a'_+,b'_+)\,d(a'_-,b'_-)=\frac{1}{\sqrt{W'_{a'_+}W'_{b'_+}W'_{a'_-}W'_{b'_-}}}\left[e^{(T_{a'}-T_{b'})}\cdot\Big(2\cosh\left(X_{a'}+X_{b'}\right)-2\cosh\left(T_{a'}+T_{b'}\right)\Big)\right]. \tag{C.10}$$

Similarly, we have

$$\begin{aligned} U'_{D_-}-U'_{S_+}&=e^{-(X_{b'}+T_{b'})}-e^{-(X_{a'}-T_{a'})}, & V'_{S_+}-V'_{D_-}&=e^{(X_{a'}+T_{a'})}-e^{(X_{b'}-T_{b'})}\,,\\ U'_{D_+}-U'_{S_-}&=e^{(X_{b'}-T_{b'})}-e^{(X_{a'}+T_{a'})}, & V'_{S_-}-V'_{D_+}&=e^{-(X_{a'}-T_{a'})}-e^{-(X_{b'}+T_{b'})}\,, \end{aligned}$$

so

$$\begin{aligned} d(a'_+,b'_-)&=\frac{1}{\sqrt{W'_{a'_+}W'_{b'_-}}}\Big[(U'_{D_-}-U'_{S_+})(V'_{S_+}-V'_{D_-})\Big]^{\frac{1}{2}}\\ &=\frac{1}{\sqrt{W'_{a'_+}W'_{b'_-}}}\left[e^{(T_{a'}-T_{b'})}\cdot\Big(2\cosh\left(X_{a'}-X_{b'}\right)-2\cosh\left(T_{a'}+T_{b'}\right)\Big)\right]^{\frac{1}{2}}, && \text{(C.11)}\\ d(a'_-,b'_+)&=\frac{1}{\sqrt{W'_{a'_-}W'_{b'_+}}}\Big[(U'_{D_+}-U'_{S_-})(V'_{S_-}-V'_{D_+})\Big]^{\frac{1}{2}}\\ &=\frac{1}{\sqrt{W'_{a'_-}W'_{b'_+}}}\left[e^{(T_{a'}-T_{b'})}\cdot\Big(2\cosh\left(X_{a'}-X_{b'}\right)-2\cosh\left(T_{a'}+T_{b'}\right)\Big)\right]^{\frac{1}{2}}. && \text{(C.12)} \end{aligned}$$

Now, putting (C.11) and (C.12) together

$$d(a'_+,b'_-)\,d(a'_-,b'_+)=\frac{1}{\sqrt{W'_{a'_+}W'_{b'_-}W'_{a'_-}W'_{b'_+}}}\left[e^{(T_{a'}-T_{b'})}\cdot\Big(2\cosh\left(X_{a'}-X_{b'}\right)-2\cosh\left(T_{a'}+T_{b'}\right)\Big)\right]. \tag{C.13}$$

Putting (C.10) and (C.13) together we get

$$\frac{c}{3}\log\frac{d(a'_+,b'_+)d(a'_-,b'_-)}{d(a'_+,b'_-)d(a'_-,b'_+)}=\frac{c}{3}\log\left[\frac{2\cosh\left(T_{a'}+T_{b'}\right)-2\cosh\left(X_{a'}+X_{b'}\right)}{2\cosh\left(T_{a'}+T_{b'}\right)-2\cosh\left(X_{a'}-X_{b'}\right)}\right]. \tag{C.14}$$

Here

$$\begin{aligned} 2\cosh\left(T_{a'}+T_{b'}\right)=\frac{1}{2}\Bigg[&\frac{(r_S-a')^{\alpha_S\beta_S}(a'+r_D+r_S)^{\alpha_S\beta_M}(b'-r_S)^{\alpha_D\beta_S}(b'+r_D+r_S)^{\alpha_D\beta_M}}{(r_D-a')^{\alpha_S\beta_D}(b'-r_D)^{\alpha_D\beta_D}}\\ &+\frac{(r_D-a')^{\alpha_S\beta_D}(b'-r_D)^{\alpha_D\beta_D}}{(b'+r_D+r_S)^{\alpha_D\beta_M}(b'-r_S)^{\alpha_D\beta_S}(r_S-a')^{\alpha_S\beta_S}(a'+r_D+r_S)^{\alpha_S\beta_M}}\Bigg]\\ \sim\frac{1}{2}\,&\frac{(b'-r_D)^{\alpha_D\beta_D}}{(r_S-a')^{\alpha_S\beta_S}}\,\frac{1}{C(a')}\,, \end{aligned} \tag{C.15}$$

using the approximation (4.2), and (4.7). Thus we obtain

$$\frac{c}{3}\log\frac{d(a_+,b'_+)d(a_-,b'_-)}{d(a_+,b'_-)d(a_-,b'_+)} = \frac{c}{3}\log\left[1-2\frac{(r_S-a')^{\alpha_S\beta_S}}{(b'-r_D)^{\alpha_D\beta_D}}\,C(a')\,\cosh\left(X_{a'}+X_{b'}\right)\right] - \frac{c}{3}\log\left[1-2\frac{(r_S-a')^{\alpha_S\beta_S}}{(b'-r_D)^{\alpha_D\beta_D}}\,C(a')\,\cosh\left(X_{a'}-X_{b'}\right)\right]. \tag{C.16}$$

The total bulk matter entanglement entropy thus is (C.7) plus (C.16), along with the area term. Thus at large values of X'_a and X'_b, after adding the area term the total entanglement entropy S_{total} becomes (4.6) i.e.

$$S_{\text{total}} \sim \frac{2\pi a'^2}{G_N} + \frac{2c}{6}\log\left[\frac{2^2\lambda}{\alpha_D\alpha_S}\sqrt{(r_S-a')(b'-r_S)}\cdot \sqrt{\frac{(r_D-a')}{l}\frac{(b'-r_D)}{l}\frac{(a'+r_S+r_D)}{l}\frac{(b'+r_S+r_D)}{l}}\sinh X_{a'}\sinh X_{b'}\right] + \frac{c}{3}\log\left[1-2\frac{(r_S-a')^{\alpha_S\beta_S}}{(b'-r_D)^{\alpha_D\beta_D}}\,C(a')\,\cosh\left(X_{a'}+X_{b'}\right)\right] - \frac{c}{3}\log\left[1-2\frac{(r_S-a')^{\alpha_S\beta_S}}{(b'-r_D)^{\alpha_D\beta_D}}\,C(a')\,\cosh\left(X_{a'}-X_{b'}\right)\right]. \tag{C.17}$$

D Inconsistencies in other island solutions

In this section, we briefly describe inconsistencies in other potential island solutions.

D.1 Island outside the black hole horizon

We discuss a potential island with boundary just outside the black hole horizon i.e. in the static diamond, similar to the results in [92] reviewed in section A. Here we use the static diamond Kruskal coordinates (2.15) redefined as $X_a = \alpha_S t_a$ and $T_a = \alpha_S r^*_a$ for the location of the island boundary. The calculation now gives the total generalized entropy as

$$S_{\text{total}} = \frac{2\pi a^2}{G_N} + \frac{c}{6}\log\left[\frac{2^4\lambda^2}{\alpha_D^2\alpha_S^2}(a-r_S)(b'-r_S)\left(\frac{r_D-a}{l}\right)\left(\frac{b'-r_D}{l}\right)\cdot \left(\frac{a+r_S+r_D}{l}\right)\left(\frac{b+r_S+r_D}{l}\right)\cosh^2 X_a\sinh^2 X_{b'}\right] + \frac{c}{3}\log\left[1+2\frac{(a-r_S)^{\alpha_S\beta_S}}{(b'-r_D)^{\alpha_D\beta_D}}\,C(a)\,\sinh\left(X_a+X_{b'}\right)\right] - \frac{c}{3}\log\left[1+2\frac{(a-r_S)^{\alpha_S\beta_S}}{(b'-r_D)^{\alpha_D\beta_D}}\,C(a)\,\sinh\left(X_a-X_{b'}\right)\right]. \tag{D.1}$$

Extremizing (D.1) with the island boundary a as $\frac{\partial S_{\rm total}}{\partial a}=0$ gives

$$\frac{4\pi a}{G_N}+\frac{c}{6}\frac{1}{a-r_S}+\frac{c}{3}\frac{C(a)}{\sqrt{b'-r_D}\sqrt{a-r_S}}\cdot\left[\frac{\sinh(X_a+X_{b'})}{1+2\frac{(a-r_S)^{\alpha_S\beta_S}}{(b'-r_D)^{\alpha_D\beta_D}}C(a)\,\sinh\left(X_a+X_{b'}\right)}\right.$$
$$\left.-\frac{\sinh(X_a-X_{b'})}{1+2\frac{(a-r_S)^{\alpha_S\beta_S}}{(b'-r_D)^{\alpha_D\beta_D}}C(a)\,\sinh\left(X_a-X_{b'}\right)}\right]=0\,. \tag{D.2}$$

Next, extremizing (D.1) with respect to X_a as $\frac{\partial S_{\rm total}}{\partial X_a}=0$ gives

$$\tanh X_a=2\sqrt{\frac{a-r_S}{b'-r_D}}\,C(a)\cdot\left[\frac{\cosh(X_a-X_{b'})}{1+2\frac{(a-r_S)^{\alpha_S\beta_S}}{(b'-r_D)^{\alpha_D\beta_D}}C(a)\,\sinh\left(X_a-X_{b'}\right)}\right.$$
$$\left.-\frac{\cosh(X_a+X_{b'})}{1+2\frac{(a-r_S)^{\alpha_S\beta_S}}{(b'-r_D)^{\alpha_D\beta_D}}C(a)\,\sinh\left(X_a+X_{b'}\right)}\right] \tag{D.3}$$

Considering $X_a=X_{b'}$, (D.3) becomes

$$1+2\sqrt{\frac{a-r_S}{b'-r_D}}C(a)\sinh 2X_a=2\sqrt{\frac{a-r_S}{b'-r_D}}C(a)\frac{1}{\tanh X_a}$$
$$\cdot\left[1+2\sqrt{\frac{a-r_S}{b'-r_D}}C(a)\sinh 2X_a-\cosh 2X_a\right]. \tag{D.4}$$

Putting this condition (D.4) back in (D.2) for large X_a (with $a-r_S$ small) gives

$$a+\frac{G_Nc}{24\pi}\frac{1}{a-r_S}\left(1-\frac{\tanh X_a}{\coth 2X_a}\right)=0\,. \tag{D.5}$$

It can be seen that $\frac{\tanh X_a}{\coth 2X_a}<1$ always so that all terms are positive here: thus there is no solution with $a>r_S$. Thus these extremization equations (D.2) and (D.3) together do not give reasonable island solutions.

Similarly, if we consider $X_a=-X_{b'}$, (D.3) becomes

$$1+2\sqrt{\frac{a-r_S}{b'-r_D}}C(a)\sinh 2X_a=2\sqrt{\frac{a-r_S}{b'-r_D}}C(a)\frac{1}{\tanh X_a}$$
$$\cdot\left[-1-2\sqrt{\frac{a-r_S}{b'-r_D}}C(a)\sinh 2X_a+\cosh 2X_a\right]. \tag{D.6}$$

Putting this condition (D.6) back in (D.2) for large X_a gives (D.5) again.

D.2 Island inside the black hole: another possibility

Recalling section 4 and the extremization equations (4.9), (4.10). Instead of $X_{a'}=X_{b'}$ considered there, let us consider $X_{a'}=-X_{b'}$: then $X_{a'}+X_{b'}=0$ and $X_{a'}-X_{b'}=2X_{a'}$. Then (4.10) gives for large $X_{a'}$ and $X_{b'}$:

$$1-2\sqrt{\frac{r_S-a'}{b'-r_D}}C(a')\cosh 2X_{a'}=-2\sqrt{\frac{r_S-a'}{b'-r_D}}C(a')\frac{\sinh 2X_{a'}}{\coth X_{a'}}\,. \tag{D.7}$$

The minus sign on the right hand side leads to trouble when this is put back in (4.9), giving no semiclassical $a'\lesssim r_S$ near horizon island solution.

E Future boundary, timelike separated QES

In this section, we exhibit other quantum extremal surface solutions which are timelike separated from the radiation region near the future boundary. We will use several technical details from [134].

The Schwarzschild de Sitter metric (2.1), after the redefinitions $\tau = \frac{l}{r}$, $\omega = \frac{t}{l}$, becomes

$$ds^2 = \frac{l^2}{\tau^2}\left(-\frac{d\tau^2}{f(\tau)}+f(\tau)d\omega^2+d\Omega_2^2\right),\; f(\tau)=1-\tau^2+\frac{2m}{l}\tau^3=(1-a_1\tau)(1-a_2\tau)(1+(a_1+a_2)\tau),$$
$$a_1a_2(a_1+a_2)=\frac{2m}{l}, \qquad a_1^2+a_1a_2+a_2^2=1; \qquad 0<a_2<a_1<1; \qquad \frac{m}{l}\leq\frac{1}{3\sqrt{3}}. \tag{E.1}$$

In the above, $\tau_c = \frac{1}{a_1}$ and $\tau_s = \frac{1}{a_2}$ are the cosmological (de Sitter) and Schwarzschild horizons. (The third zero does not correspond to a physical horizon.)

For SdS_4 with $f(\tau)$ in (E.1), the tortoise coordinate $y = \int \frac{d\tau}{f(\tau)}$ can be defined as

$$y = \int \frac{d\tau}{1-\tau^2+\frac{2m}{l}\tau^3} = -\beta_1\log(1-a_1\tau)+\beta_2\log(1-a_2\tau)+\beta_3\log(1+(a_1+a_2)\tau)\,. \tag{E.2}$$

With the parameters

$$\beta_1 = \frac{a_1}{3a_1^2-1}, \qquad \beta_2 = -\frac{a_2}{3a_2^2-1}, \qquad \beta_3 = \frac{a_1+a_2}{3a_1a_2+2} \tag{E.3}$$

the SdS_4 metric becomes

$$ds^2 = l^2\left(\frac{1}{\tau^2}-1+\frac{2m}{l}\tau\right)(d\omega^2-dy^2)+\frac{l^2}{\tau^2}d\Omega_2^2\,. \tag{E.4}$$

Now, we consider the same reduction ansatz from [92] to perform dimentional reduction of the SdS_4 background to 2-dimensions. The 2-dim metric and dilaton become

$$ds_2^2 = \frac{\lambda l^3}{\tau}\left(\frac{1}{\tau^2}-1+\frac{2m}{l}\tau\right)(d\omega^2-dy^2), \qquad \phi = \phi_r\frac{\lambda^2 l^2}{\tau^2}\,. \tag{E.5}$$

In the reduced 2-dim Schwarzschild de sitter spacetime,the Kruskal coordinates around the cosmological horizon are then defined as U, V and the metric becomes

$$U = e^{\frac{\omega-y}{2\beta_1}}, \quad V = -e^{-\frac{\omega+y}{2\beta_1}}; \qquad UV = -e^{-\frac{y}{\beta_1}}, \quad \frac{U}{V} = -e^{\frac{\omega}{\beta_1}};$$
$$UV = (a_1\tau-1)(1-a_2\tau)^{-\frac{\beta_2}{\beta_1}}(1+(a_1+a_2)\tau)^{-\frac{\beta_3}{\beta_1}}\,, \tag{E.6}$$
$$ds_2^2 = \frac{4\beta_1^2 g(U,V)}{UV}\,dUdV\,. \tag{E.7}$$

Using (E.5), the generalized entropy for a future boundary observer at $(\omega,\tau)=(\omega_0,\tau_0)$ in the 2-dim SdS_4 spacetime becomes (with $P(\tau_0) = \frac{1}{\tau_0^2}-1+\frac{2m}{l}\tau_0$)

$$S_{\text{gen}} = \frac{\phi_r}{4G}\frac{l^2}{\tau^2}+\frac{c}{12}\log\left[\frac{1}{\epsilon_{\text{uv}}^4}((\omega-\omega_0)^2-(y-y_0)^2)^2\frac{\lambda^2 l^6}{\tau\tau_0}P(\tau_0)\left(\frac{1}{\tau^2}-1+\frac{2m}{l}\tau\right)\right]. \tag{E.8}$$

This expression for $S_{\rm gen}$ should be regarded as a smooth function of U, V, with respect to which we will extremize to find quantum extremal surfaces. However the nature of the QES here can be gleaned by simply noting that the only place the spatial future boundary coordinate ω enters is through the spacetime interval $\Delta^2 = (\omega - \omega_0)^2 - (y - y_0)^2$ inside the logarithm. Thus we expect $\frac{\partial S_{\rm gen}}{\partial \omega} = \frac{c}{3}\frac{\omega-\omega_0}{\Delta^2} = 0$, so that $\omega = \omega_0$, i.e. the QES is timelike separated from the future boundary observer.

Analysing more carefully, extremizing (E.8) with Kruskal U, V, as

$$\frac{\partial S_{\rm gen}}{\partial U} = \frac{\partial S_{\rm gen}}{\partial \tau}\frac{\partial \tau}{\partial U} + \frac{\partial S_{\rm gen}}{\partial \omega}\frac{\partial \omega}{\partial U} = 0\,, \qquad \frac{\partial S_{\rm gen}}{\partial V} = \frac{\partial S_{\rm gen}}{\partial \tau}\frac{\partial \tau}{\partial V} + \frac{\partial S_{\rm gen}}{\partial \omega}\frac{\partial \omega}{\partial V} = 0\,, \tag{E.9}$$

and, from (E.8), (E.6), (E.7), noting that

$$\frac{\partial S_{\rm gen}}{\partial \tau} = -\frac{\phi_r}{2G}\frac{l^2}{\tau^3} + \frac{c}{12}\frac{1}{f(\tau)}\left[-\frac{4(y-y_0)}{\Delta^2} + \tau\left(1 - \frac{3}{\tau^2}\right)\right], \qquad \frac{\partial S_{\rm gen}}{\partial \omega} = \frac{c}{3}\frac{\omega - \omega_0}{\Delta^2}; \tag{E.10}$$

we find the extremization conditions become

$$\left[-\frac{\phi_r}{2G}\frac{l^2}{\tau^3} + \frac{c}{12}\frac{1}{f(\tau)}\left(-\frac{4(y-y_0)}{\Delta^2} + \tau\left(1 - \frac{3}{\tau^2}\right)\right)\right]\frac{A(\tau)}{U} + \frac{c}{3}\frac{\omega - \omega_0}{\Delta^2}\frac{\beta_1}{U} = 0\,, \tag{E.11}$$

and

$$\left[-\frac{\phi_r}{2G}\frac{l^2}{\tau^3} + \frac{c}{12}\frac{1}{f(\tau)}\left(-\frac{4(y-y_0)}{\Delta^2} + \tau\left(1 - \frac{3}{\tau^2}\right)\right)\right]\frac{A(\tau)}{V} + \frac{c}{3}\frac{\omega - \omega_0}{\Delta^2}\left(-\frac{\beta_1}{V}\right) = 0\,. \tag{E.12}$$

Subtracting as (E.11)–(E.12) gives $\frac{2c}{3}\frac{\omega-\omega_0}{\Delta^2}\beta_1 = 0$. Thus,

$$\omega = \omega_0\,, \tag{E.13}$$

giving timelike separated QES with respect to the future boundary observer. The timelike separation implies that the generalized entropy becomes complex-valued, with $\log(-|\Delta^2|)$ giving rise to $\log(-1) = i\pi$, as in pure de Sitter.

Now, by putting $\omega = \omega_0$ in (E.11) gives

$$-\frac{\phi_r}{2G}\frac{l^2}{\tau^3} + \frac{c}{12}\frac{1}{f(\tau)}\left(\frac{4}{y - y_0} + \tau\left(1 - \frac{3}{\tau^2}\right)\right) = 0 \tag{E.14}$$

The future boundary observer has $r = \infty$ and $\tau_0 = 0$ so $y_0 = 0$. Further considering $\tau = 1 - \epsilon$, where $\epsilon \ll 1$, and noting $1 \ll c \ll \frac{1}{G}$, we simplify (E.14) ignoring appropriate terms and obtain

$$\frac{2c}{\log\left[\frac{(1-a_2(1-\epsilon))^{\beta_2}(1+(a_1+a_2)(1-\epsilon))^{\beta_3}}{(1-a_1(1-\epsilon))^{\beta_1}}\right]} \approx \frac{3\phi_r}{G}l^2\left[\frac{\epsilon(2-\epsilon)}{(1-\epsilon)^3} + \frac{2m}{l}\right] \tag{E.15}$$

Now, considering a_1 and a_2 perturbatively as $a_1 \simeq 1 - \frac{m}{l}$, $a_2 \simeq \frac{2m}{l}$, and $0 < a_2 < a_1 < 1$, we can obtain the parameters $\beta_1, \beta_2, \beta_3$ using (E.3) perturbatively as well. This finally gives

$$c \approx \frac{3\phi_r}{2G}l^2\left(\epsilon + \frac{m}{l}\right)\log\left(\frac{2}{\epsilon + \frac{m}{l}}\right) \tag{E.16}$$

which is a consistency condition on the central charge (number of degrees of freedom) of the 2-dim CFT matter for the timelike extremal surface to exist (pure dS corresponds to $m = 0$).

JHEP05(2024)016

References

[1] S.W. Hawking, *Breakdown of Predictability in Gravitational Collapse*, *Phys. Rev. D* **14** (1976) 2460 [INSPIRE].

[2] S.W. Hawking, *Particle Creation by Black Holes*, *Commun. Math. Phys.* **43** (1975) 199 [*Erratum ibid.* **46** (1976) 206] [INSPIRE].

[3] S.D. Mathur, *The Information paradox: A Pedagogical introduction*, *Class. Quant. Grav.* **26** (2009) 224001 [arXiv:0909.1038] [INSPIRE].

[4] A. Almheiri, D. Marolf, J. Polchinski and J. Sully, *Black Holes: Complementarity or Firewalls?*, *JHEP* **02** (2013) 062 [arXiv:1207.3123] [INSPIRE].

[5] D.N. Page, *Information in black hole radiation*, *Phys. Rev. Lett.* **71** (1993) 3743 [hep-th/9306083] [INSPIRE].

[6] D.N. Page, *Time Dependence of Hawking Radiation Entropy*, *JCAP* **09** (2013) 028 [arXiv:1301.4995] [INSPIRE].

[7] G. Penington, *Entanglement Wedge Reconstruction and the Information Paradox*, *JHEP* **09** (2020) 002 [arXiv:1905.08255] [INSPIRE].

[8] A. Almheiri, N. Engelhardt, D. Marolf and H. Maxfield, *The entropy of bulk quantum fields and the entanglement wedge of an evaporating black hole*, *JHEP* **12** (2019) 063 [arXiv:1905.08762] [INSPIRE].

[9] A. Almheiri, R. Mahajan, J. Maldacena and Y. Zhao, *The Page curve of Hawking radiation from semiclassical geometry*, *JHEP* **03** (2020) 149 [arXiv:1908.10996] [INSPIRE].

[10] G. Penington, S.H. Shenker, D. Stanford and Z. Yang, *Replica wormholes and the black hole interior*, *JHEP* **03** (2022) 205 [arXiv:1911.11977] [INSPIRE].

[11] A. Almheiri et al., *Replica Wormholes and the Entropy of Hawking Radiation*, *JHEP* **05** (2020) 013 [arXiv:1911.12333] [INSPIRE].

[12] T. Faulkner, A. Lewkowycz and J. Maldacena, *Quantum corrections to holographic entanglement entropy*, *JHEP* **11** (2013) 074 [arXiv:1307.2892] [INSPIRE].

[13] N. Engelhardt and A.C. Wall, *Quantum Extremal Surfaces: Holographic Entanglement Entropy beyond the Classical Regime*, *JHEP* **01** (2015) 073 [arXiv:1408.3203] [INSPIRE].

[14] S. Ryu and T. Takayanagi, *Holographic derivation of entanglement entropy from AdS/CFT*, *Phys. Rev. Lett.* **96** (2006) 181602 [hep-th/0603001] [INSPIRE].

[15] S. Ryu and T. Takayanagi, *Aspects of Holographic Entanglement Entropy*, *JHEP* **08** (2006) 045 [hep-th/0605073] [INSPIRE].

[16] V.E. Hubeny, M. Rangamani and T. Takayanagi, *A covariant holographic entanglement entropy proposal*, *JHEP* **07** (2007) 062 [arXiv:0705.0016] [INSPIRE].

[17] M. Rangamani and T. Takayanagi, *Holographic Entanglement Entropy*, Springer (2017) [DOI:10.1007/978-3-319-52573-0] [INSPIRE].

[18] A. Almheiri et al., *The entropy of Hawking radiation*, Rev. Mod. Phys. **93** (2021) 035002 [arXiv:2006.06872] [INSPIRE].

[19] S. Raju, *Lessons from the information paradox*, Phys. Rept. **943** (2022) 1 [arXiv:2012.05770] [INSPIRE].

[20] B. Chen, B. Czech and Z.-Z. Wang, *Quantum information in holographic duality*, Rept. Prog. Phys. **85** (2022) 046001 [arXiv:2108.09188] [INSPIRE].

[21] A. Almheiri, R. Mahajan and J. Maldacena, *Islands outside the horizon*, arXiv:1910.11077 [INSPIRE].

[22] H.Z. Chen et al., *Information Flow in Black Hole Evaporation*, JHEP **03** (2020) 152 [arXiv:1911.03402] [INSPIRE].

[23] A. Almheiri, R. Mahajan and J.E. Santos, *Entanglement islands in higher dimensions*, SciPost Phys. **9** (2020) 001 [arXiv:1911.09666] [INSPIRE].

[24] F.F. Gautason, L. Schneiderbauer, W. Sybesma and L. Thorlacius, *Page Curve for an Evaporating Black Hole*, JHEP **05** (2020) 091 [arXiv:2004.00598] [INSPIRE].

[25] T. Anegawa and N. Iizuka, *Notes on islands in asymptotically flat 2d dilaton black holes*, JHEP **07** (2020) 036 [arXiv:2004.01601] [INSPIRE].

[26] K. Hashimoto, N. Iizuka and Y. Matsuo, *Islands in Schwarzschild black holes*, JHEP **06** (2020) 085 [arXiv:2004.05863] [INSPIRE].

[27] T. Hartman, E. Shaghoulian and A. Strominger, *Islands in Asymptotically Flat 2D Gravity*, JHEP **07** (2020) 022 [arXiv:2004.13857] [INSPIRE].

[28] T.J. Hollowood and S.P. Kumar, *Islands and Page Curves for Evaporating Black Holes in JT Gravity*, JHEP **08** (2020) 094 [arXiv:2004.14944] [INSPIRE].

[29] C. Krishnan, V. Patil and J. Pereira, *Page Curve and the Information Paradox in Flat Space*, arXiv:2005.02993 [INSPIRE].

[30] M. Alishahiha, A. Faraji Astaneh and A. Naseh, *Island in the presence of higher derivative terms*, JHEP **02** (2021) 035 [arXiv:2005.08715] [INSPIRE].

[31] H. Geng and A. Karch, *Massive islands*, JHEP **09** (2020) 121 [arXiv:2006.02438] [INSPIRE].

[32] T. Li, J. Chu and Y. Zhou, *Reflected Entropy for an Evaporating Black Hole*, JHEP **11** (2020) 155 [arXiv:2006.10846] [INSPIRE].

[33] X. Dong, X.-L. Qi, Z. Shangnan and Z. Yang, *Effective entropy of quantum fields coupled with gravity*, JHEP **10** (2020) 052 [arXiv:2007.02987] [INSPIRE].

[34] H.Z. Chen et al., *Evaporating Black Holes Coupled to a Thermal Bath*, JHEP **01** (2021) 065 [arXiv:2007.11658] [INSPIRE].

[35] Y. Ling, Y. Liu and Z.-Y. Xian, *Island in Charged Black Holes*, JHEP **03** (2021) 251 [arXiv:2010.00037] [INSPIRE].

[36] Y. Matsuo, *Islands and stretched horizon*, JHEP **07** (2021) 051 [arXiv:2011.08814] [INSPIRE].

[37] K. Goto, T. Hartman and A. Tajdini, *Replica wormholes for an evaporating 2D black hole*, JHEP **04** (2021) 289 [arXiv:2011.09043] [INSPIRE].

[38] I. Akal et al., *Entanglement Entropy in a Holographic Moving Mirror and the Page Curve*, Phys. Rev. Lett. **126** (2021) 061604 [arXiv:2011.12005] [INSPIRE].

JHEP05(2024)016

[39] H. Geng et al., *Information Transfer with a Gravitating Bath*, *SciPost Phys.* **10** (2021) 103 [arXiv:2012.04671] [INSPIRE].

[40] F. Deng, J. Chu and Y. Zhou, *Defect extremal surface as the holographic counterpart of Island formula*, *JHEP* **03** (2021) 008 [arXiv:2012.07612] [INSPIRE].

[41] G.K. Karananas, A. Kehagias and J. Taskas, *Islands in linear dilaton black holes*, *JHEP* **03** (2021) 253 [arXiv:2101.00024] [INSPIRE].

[42] X. Wang, R. Li and J. Wang, *Islands and Page curves of Reissner-Nordström black holes*, *JHEP* **04** (2021) 103 [arXiv:2101.06867] [INSPIRE].

[43] E. Verheijden and E. Verlinde, *From the BTZ black hole to JT gravity: geometrizing the island*, *JHEP* **11** (2021) 092 [arXiv:2102.00922] [INSPIRE].

[44] K. Kawabata, T. Nishioka, Y. Okuyama and K. Watanabe, *Probing Hawking radiation through capacity of entanglement*, *JHEP* **05** (2021) 062 [arXiv:2102.02425] [INSPIRE].

[45] L. Anderson, O. Parrikar and R.M. Soni, *Islands with gravitating baths: towards ER = EPR*, *JHEP* **10** (2020) 226 [arXiv:2103.14746] [INSPIRE].

[46] A. Bhattacharya, A. Bhattacharyya, P. Nandy and A.K. Patra, *Islands and complexity of eternal black hole and radiation subsystems for a doubly holographic model*, *JHEP* **05** (2021) 135 [arXiv:2103.15852] [INSPIRE].

[47] W. Kim and M. Nam, *Entanglement entropy of asymptotically flat non-extremal and extremal black holes with an island*, *Eur. Phys. J. C* **81** (2021) 869 [arXiv:2103.16163] [INSPIRE].

[48] K. Ghosh and C. Krishnan, *Dirichlet baths and the not-so-fine-grained Page curve*, *JHEP* **08** (2021) 119 [arXiv:2103.17253] [INSPIRE].

[49] X. Wang, R. Li and J. Wang, *Page curves for a family of exactly solvable evaporating black holes*, *Phys. Rev. D* **103** (2021) 126026 [arXiv:2104.00224] [INSPIRE].

[50] R. Li, X. Wang and J. Wang, *Island may not save the information paradox of Liouville black holes*, *Phys. Rev. D* **104** (2021) 106015 [arXiv:2105.03271] [INSPIRE].

[51] R. Li and J. Wang, *Hawking radiation and page curves of the black holes in thermal environment*, *Commun. Theor. Phys.* **73** (2021) 075401 [INSPIRE].

[52] K. Kawabata, T. Nishioka, Y. Okuyama and K. Watanabe, *Replica wormholes and capacity of entanglement*, *JHEP* **10** (2021) 227 [arXiv:2105.08396] [INSPIRE].

[53] Y. Lu and J. Lin, *Islands in Kaluza-Klein black holes*, *Eur. Phys. J. C* **82** (2022) 132 [arXiv:2106.07845] [INSPIRE].

[54] J. Kruthoff, R. Mahajan and C. Murdia, *Free fermion entanglement with a semitransparent interface: the effect of graybody factors on entanglement islands*, *SciPost Phys.* **11** (2021) 063 [arXiv:2106.10287] [INSPIRE].

[55] M.-H. Yu and X.-H. Ge, *Islands and Page curves in charged dilaton black holes*, *Eur. Phys. J. C* **82** (2022) 14 [arXiv:2107.03031] [INSPIRE].

[56] B. Ahn et al., *Islands in charged linear dilaton black holes*, *Phys. Rev. D* **105** (2022) 046012 [arXiv:2107.07444] [INSPIRE].

[57] X. Wang, K. Zhang and J. Wang, *What can we learn about islands and state paradox from quantum information theory?*, arXiv:2107.09228 [INSPIRE].

[58] I. Aref'eva and I. Volovich, *A note on islands in Schwarzschild black holes*, *Teor. Mat. Fiz.* **214** (2023) 500 [arXiv:2110.04233] [INSPIRE].

[59] S. He, Y. Sun, L. Zhao and Y.-X. Zhang, *The universality of islands outside the horizon*, *JHEP* **05** (2022) 047 [arXiv:2110.07598] [INSPIRE].

[60] Y. Matsuo, *Entanglement entropy and vacuum states in Schwarzschild geometry*, *JHEP* **06** (2022) 109 [arXiv:2110.13898] [INSPIRE].

[61] F. Omidi, *Entropy of Hawking radiation for two-sided hyperscaling violating black branes*, *JHEP* **04** (2022) 022 [arXiv:2112.05890] [INSPIRE].

[62] R. Espíndola, B. Najian and D. Nikolakopoulou, *Islands in FRW Cosmologies*, arXiv:2203.04433 [INSPIRE].

[63] J. Tian, *Islands in Generalized Dilaton Theories*, *Symmetry* **15** (2023) 1402 [arXiv:2204.08751] [INSPIRE].

[64] A. Laddha, S.G. Prabhu, S. Raju and P. Shrivastava, *The Holographic Nature of Null Infinity*, *SciPost Phys.* **10** (2021) 041 [arXiv:2002.02448] [INSPIRE].

[65] H. Geng et al., *Inconsistency of islands in theories with long-range gravity*, *JHEP* **01** (2022) 182 [arXiv:2107.03390] [INSPIRE].

[66] I. Bena, E.J. Martinec, S.D. Mathur and N.P. Warner, *Fuzzballs and Microstate Geometries: Black-Hole Structure in String Theory*, arXiv:2204.13113 [INSPIRE].

[67] C. Krishnan, *Critical Islands*, *JHEP* **01** (2021) 179 [arXiv:2007.06551] [INSPIRE].

[68] Y. Chen, V. Gorbenko and J. Maldacena, *Bra-ket wormholes in gravitationally prepared states*, *JHEP* **02** (2021) 009 [arXiv:2007.16091] [INSPIRE].

[69] T. Hartman, Y. Jiang and E. Shaghoulian, *Islands in cosmology*, *JHEP* **11** (2020) 111 [arXiv:2008.01022] [INSPIRE].

[70] M. Van Raamsdonk, *Comments on wormholes, ensembles, and cosmology*, *JHEP* **12** (2021) 156 [arXiv:2008.02259] [INSPIRE].

[71] V. Balasubramanian, A. Kar and T. Ugajin, *Islands in de Sitter space*, *JHEP* **02** (2021) 072 [arXiv:2008.05275] [INSPIRE].

[72] W. Sybesma, *Pure de Sitter space and the island moving back in time*, *Class. Quant. Grav.* **38** (2021) 145012 [arXiv:2008.07994] [INSPIRE].

[73] A. Manu, K. Narayan and P. Paul, *Cosmological singularities, entanglement and quantum extremal surfaces*, *JHEP* **04** (2021) 200 [arXiv:2012.07351] [INSPIRE].

[74] S. Choudhury et al., *Circuit Complexity from Cosmological Islands*, *Symmetry* **13** (2021) 1301 [arXiv:2012.10234] [INSPIRE].

[75] R. Bousso and A. Shahbazi-Moghaddam, *Island Finder and Entropy Bound*, *Phys. Rev. D* **103** (2021) 106005 [arXiv:2101.11648] [INSPIRE].

[76] H. Geng, Y. Nomura and H.-Y. Sun, *Information paradox and its resolution in de Sitter holography*, *Phys. Rev. D* **103** (2021) 126004 [arXiv:2103.07477] [INSPIRE].

[77] S. Fallows and S.F. Ross, *Islands and mixed states in closed universes*, *JHEP* **07** (2021) 022 [arXiv:2103.14364] [INSPIRE].

[78] L. Aalsma and W. Sybesma, *The Price of Curiosity: Information Recovery in de Sitter Space*, *JHEP* **05** (2021) 291 [arXiv:2104.00006] [INSPIRE].

[79] C.F. Uhlemann, *Islands and Page curves in 4d from Type IIB*, *JHEP* **08** (2021) 104 [arXiv:2105.00008] [INSPIRE].

JHEP05(2024)016

[80] D. Giataganas and N. Tetradis, *Entanglement entropy in FRW backgrounds*, *Phys. Lett. B* **820** (2021) 136493 [arXiv:2105.12614] [INSPIRE].

[81] L. Aalsma et al., *Shocks and information exchange in de Sitter space*, *JHEP* **10** (2021) 104 [arXiv:2105.12737] [INSPIRE].

[82] K. Langhoff, C. Murdia and Y. Nomura, *Multiverse in an inverted island*, *Phys. Rev. D* **104** (2021) 086007 [arXiv:2106.05271] [INSPIRE].

[83] S.E. Aguilar-Gutierrez et al., *Islands in Multiverse Models*, *JHEP* **05** (2021) 137 [*Addendum ibid.* **05** (2022) 137] [arXiv:2108.01278] [INSPIRE].

[84] E. Shaghoulian, *The central dogma and cosmological horizons*, *JHEP* **01** (2022) 132 [arXiv:2110.13210] [INSPIRE].

[85] C.-J. Chou, H.B. Lao and Y. Yang, *Page curve of effective Hawking radiation*, *Phys. Rev. D* **106** (2022) 066008 [arXiv:2111.14551] [INSPIRE].

[86] K. Goswami, K. Narayan and H.K. Saini, *Cosmologies, singularities and quantum extremal surfaces*, *JHEP* **03** (2022) 201 [arXiv:2111.14906] [INSPIRE].

[87] R. Bousso and E. Wildenhain, *Islands in closed and open universes*, *Phys. Rev. D* **105** (2022) 086012 [arXiv:2202.05278] [INSPIRE].

[88] U. Moitra, S.K. Sake and S.P. Trivedi, *Aspects of Jackiw-Teitelboim gravity in Anti-de Sitter and de Sitter spacetime*, *JHEP* **06** (2022) 138 [arXiv:2202.03130] [INSPIRE].

[89] A. Svesko, E. Verheijden, E.P. Verlinde and M.R. Visser, *Quasi-local energy and microcanonical entropy in two-dimensional nearly de Sitter gravity*, *JHEP* **08** (2022) 075 [arXiv:2203.00700] [INSPIRE].

[90] D.S. Ageev and I.Y. Aref'eva, *Thermal density matrix breaks down the Page curve*, *Eur. Phys. J. Plus* **137** (2022) 1188 [arXiv:2206.04094] [INSPIRE].

[91] A. Karch, H. Sun and C.F. Uhlemann, *Double holography in string theory*, *JHEP* **10** (2022) 012 [arXiv:2206.11292] [INSPIRE].

[92] K. Goswami and K. Narayan, *Small Schwarzschild de Sitter black holes, quantum extremal surfaces and islands*, *JHEP* **10** (2022) 031 [arXiv:2207.10724] [INSPIRE].

[93] A. Roy Chowdhury, A. Saha and S. Gangopadhyay, *Role of mutual information in the Page curve*, *Phys. Rev. D* **106** (2022) 086019 [arXiv:2207.13029] [INSPIRE].

[94] M.-H. Yu and X.-H. Ge, *Entanglement islands in generalized two-dimensional dilaton black holes*, *Phys. Rev. D* **107** (2023) 066020 [arXiv:2208.01943] [INSPIRE].

[95] R. Bousso and G. Penington, *Entanglement wedges for gravitating regions*, *Phys. Rev. D* **107** (2023) 086002 [arXiv:2208.04993] [INSPIRE].

[96] P.-J. Hu, D. Li and R.-X. Miao, *Island on codimension-two branes in AdS/dCFT*, *JHEP* **11** (2022) 008 [arXiv:2208.11982] [INSPIRE].

[97] D.S. Ageev et al., *Infrared regularization and finite size dynamics of entanglement entropy in Schwarzschild black hole*, *Phys. Rev. D* **108** (2023) 046005 [arXiv:2209.00036] [INSPIRE].

[98] C.-S. Chu and R.-X. Miao, *Tunneling of Bell Particles, Page Curve and Black Hole Information*, arXiv:2209.03610 [INSPIRE].

[99] G. Yadav and N. Joshi, *Cosmological and black hole islands in multi-event horizon spacetimes*, *Phys. Rev. D* **107** (2023) 026009 [arXiv:2210.00331] [INSPIRE].

JHEP05(2024)016

[100] L. Aalsma, S.E. Aguilar-Gutierrez and W. Sybesma, *An outsider's perspective on information recovery in de Sitter space*, *JHEP* **01** (2023) 129 [arXiv:2210.12176] [INSPIRE].

[101] C.-Y. Lu, M.-H. Yu, X.-H. Ge and L.-J. Tian, *Page curve and phase transition in deformed Jackiw-Teitelboim gravity*, *Eur. Phys. J. C* **83** (2023) 215 [arXiv:2210.14750] [INSPIRE].

[102] D. Stepanenko and I. Volovich, *Schwarzschild black holes, Islands and Virasoro algebra*, *Eur. Phys. J. Plus* **138** (2023) 688 [arXiv:2211.03153] [INSPIRE].

[103] I. Ben-Dayan, M. Hadad and E. Wildenhain, *Islands in the fluid: islands are common in cosmology*, *JHEP* **03** (2023) 077 [arXiv:2211.16600] [INSPIRE].

[104] D. Basu, Q. Wen and S. Zhou, *Entanglement Islands from Hilbert Space Reduction*, arXiv:2211.17004 [INSPIRE].

[105] J. Kudler-Flam and Y. Kusuki, *On quantum information before the Page time*, *JHEP* **05** (2023) 078 [arXiv:2212.06839] [INSPIRE].

[106] R. Emparan et al., *Holographic duals of evaporating black holes*, *JHEP* **05** (2023) 182 [arXiv:2301.02587] [INSPIRE].

[107] Y.-S. Piao, *Implication of the island rule for inflation and primordial perturbations*, *Phys. Rev. D* **107** (2023) 123509 [arXiv:2301.07403] [INSPIRE].

[108] C.-Z. Guo, W.-C. Gan and F.-W. Shu, *Page curves and entanglement islands for the step-function Vaidya model of evaporating black holes*, *JHEP* **05** (2023) 042 [arXiv:2302.02379] [INSPIRE].

[109] S. Parvizi and M. Shahbazi, *Analogue gravity and the island prescription*, *Eur. Phys. J. C* **83** (2023) 705 [arXiv:2302.08742] [INSPIRE].

[110] T.N. Hung and C.H. Nam, *Compactified extra dimension and entanglement island as clues to quantum gravity*, *Eur. Phys. J. C* **83** (2023) 472 [arXiv:2303.00348] [INSPIRE].

[111] C.-H. Wu and J. Xu, *Islands in non-minimal dilaton gravity: exploring effective theories for black hole evaporation*, *JHEP* **10** (2023) 094 [arXiv:2303.03410] [INSPIRE].

[112] M. Cadoni, M. Oi and A.P. Sanna, *Evaporation and information puzzle for 2D nonsingular asymptotically flat black holes*, *JHEP* **06** (2023) 211 [arXiv:2303.05557] [INSPIRE].

[113] A. Roy Chowdhury, A. Saha and S. Gangopadhyay, *Mutual information of subsystems and the Page curve for the Schwarzschild-de Sitter black hole*, *Phys. Rev. D* **108** (2023) 026003 [arXiv:2303.14062] [INSPIRE].

[114] D.S. Ageev et al., *Entanglement entropy in de Sitter: no pure states for conformal matter*, arXiv:2304.12351 [INSPIRE].

[115] D. Basu, J. Lin, Y. Lu and Q. Wen, *Ownerless island and partial entanglement entropy in island phases*, *SciPost Phys.* **15** (2023) 227 [arXiv:2305.04259] [INSPIRE].

[116] H.-S. Jeong, K.-Y. Kim and Y.-W. Sun, *Entanglement entropy analysis of dyonic black holes using doubly holographic theory*, *Phys. Rev. D* **108** (2023) 126016 [arXiv:2305.18122] [INSPIRE].

[117] C.-W. Tong, D.-H. Du and J.-R. Sun, *Island of Reissner-Nordström anti-de Sitter black holes in the large d limit*, arXiv:2306.06682 [INSPIRE].

[118] M.-H. Yu, X.-H. Ge and C.-Y. Lu, *Page curves for accelerating black holes*, *Eur. Phys. J. C* **83** (2023) 1104 [arXiv:2306.11407] [INSPIRE].

JHEP05(2024)016

[119] C.-J. Chou, H.B. Lao and Y. Yang, *Page Curve of AdS-Vaidya Model for Evaporating Black Holes*, arXiv:2306.16744 [INSPIRE].

[120] S.E. Aguilar-Gutierrez, R. Espíndola and E.K. Morvan-Benhaim, *A teleportation protocol in Schwarzschild-de Sitter space*, arXiv:2308.13516 [INSPIRE].

[121] B. Czech, S. Shuai and H. Tang, *Entropies and reflected entropies in the Hayden-Preskill protocol*, *JHEP* **02** (2024) 040 [arXiv:2310.16988] [INSPIRE].

[122] V. Franken, H. Partouche, F. Rondeau and N. Toumbas, *Closed FRW holography: A time-dependent ER=EPR realization*, arXiv:2310.20652 [INSPIRE].

[123] K. Narayan, *Extremal surfaces in de Sitter spacetime*, *Phys. Rev. D* **91** (2015) 126011 [arXiv:1501.03019] [INSPIRE].

[124] Y. Sato, *Comments on Entanglement Entropy in the dS/CFT Correspondence*, *Phys. Rev. D* **91** (2015) 086009 [arXiv:1501.04903] [INSPIRE].

[125] K. Narayan, *On extremal surfaces and de Sitter entropy*, *Phys. Lett. B* **779** (2018) 214 [arXiv:1711.01107] [INSPIRE].

[126] K. Doi et al., *Pseudoentropy in dS/CFT and Timelike Entanglement Entropy*, *Phys. Rev. Lett.* **130** (2023) 031601 [arXiv:2210.09457] [INSPIRE].

[127] K. Narayan, *de Sitter space, extremal surfaces, and time entanglement*, *Phys. Rev. D* **107** (2023) 126004 [arXiv:2210.12963] [INSPIRE].

[128] G.W. Gibbons and S.W. Hawking, *Cosmological Event Horizons, Thermodynamics, and Particle Creation*, *Phys. Rev. D* **15** (1977) 2738 [INSPIRE].

[129] P.H. Ginsparg and M.J. Perry, *Semiclassical Perdurance of de Sitter Space*, *Nucl. Phys. B* **222** (1983) 245 [INSPIRE].

[130] R. Bousso and S.W. Hawking, *Pair creation of black holes during inflation*, *Phys. Rev. D* **54** (1996) 6312 [gr-qc/9606052] [INSPIRE].

[131] R. Bousso and S.W. Hawking, *(Anti)evaporation of Schwarzschild-de Sitter black holes*, *Phys. Rev. D* **57** (1998) 2436 [hep-th/9709224] [INSPIRE].

[132] H. Nariai, *On some static solutions of Einstein's gravitational field equations in a spherically symmetric case*, *Sci. Rep. Tóhoku Univ.* **34** (1950) 160.

[133] J. Maldacena, G.J. Turiaci and Z. Yang, *Two dimensional Nearly de Sitter gravity*, *JHEP* **01** (2021) 139 [arXiv:1904.01911] [INSPIRE].

[134] K. Fernandes, K.S. Kolekar, K. Narayan and S. Roy, *Schwarzschild de Sitter and extremal surfaces*, *Eur. Phys. J. C* **80** (2020) 866 [arXiv:1910.11788] [INSPIRE].

[135] S. Shankaranarayanan, *Temperature and entropy of Schwarzschild-de Sitter space-time*, *Phys. Rev. D* **67** (2003) 084026 [gr-qc/0301090] [INSPIRE].

[136] J. Guven and D. Núñez, *Schwarzschild-de Sitter space and its perturbations*, *Phys. Rev. D* **42** (1990) 2577 [INSPIRE].

[137] A. Strominger, *Les Houches lectures on black holes*, in the proceedings of the *NATO Advanced Study Institute: Les Houches Summer School, Session 62: Fluctuating Geometries in Statistical Mechanics and Field Theory*, Les Houches, France, 2 August–9 September 1994 [hep-th/9501071] [INSPIRE].

[138] D. Grumiller, W. Kummer and D.V. Vassilevich, *Dilaton gravity in two-dimensions*, *Phys. Rept.* **369** (2002) 327 [hep-th/0204253] [INSPIRE].

JHEP05(2024)016

[139] T.G. Mertens and G.J. Turiaci, *Solvable models of quantum black holes: a review on Jackiw-Teitelboim gravity*, Living Rev. Rel. **26** (2023) 4 [arXiv:2210.10846] [INSPIRE].

[140] K. Narayan, *Aspects of two-dimensional dilaton gravity, dimensional reduction, and holography*, Phys. Rev. D **104** (2021) 026007 [arXiv:2010.12955] [INSPIRE].

[141] R. Bhattacharya, K. Narayan and P. Paul, *Cosmological singularities and 2-dimensional dilaton gravity*, JHEP **08** (2020) 062 [arXiv:2006.09470] [INSPIRE].

[142] P. Calabrese and J.L. Cardy, *Entanglement entropy and quantum field theory*, J. Stat. Mech. **0406** (2004) P06002 [hep-th/0405152] [INSPIRE].

[143] P. Calabrese and J. Cardy, *Entanglement entropy and conformal field theory*, J. Phys. A **42** (2009) 504005 [arXiv:0905.4013] [INSPIRE].

[144] L. Susskind, *The Census taker's hat*, arXiv:0710.1129 [INSPIRE].

[145] P. Calabrese, J. Cardy and E. Tonni, *Entanglement entropy of two disjoint intervals in conformal field theory*, J. Stat. Mech. **0911** (2009) P11001 [arXiv:0905.2069] [INSPIRE].

[146] P. Calabrese, J. Cardy and E. Tonni, *Entanglement entropy of two disjoint intervals in conformal field theory II*, J. Stat. Mech. **1101** (2011) P01021 [arXiv:1011.5482] [INSPIRE].

[147] M. Headrick, *Entanglement Renyi entropies in holographic theories*, Phys. Rev. D **82** (2010) 126010 [arXiv:1006.0047] [INSPIRE].

[148] J.F. Pedraza, A. Svesko, W. Sybesma and M.R. Visser, *Semi-classical thermodynamics of quantum extremal surfaces in Jackiw-Teitelboim gravity*, JHEP **12** (2021) 134 [arXiv:2107.10358] [INSPIRE].

[149] J.F. Pedraza, A. Svesko, W. Sybesma and M.R. Visser, *Microcanonical action and the entropy of Hawking radiation*, Phys. Rev. D **105** (2022) 126010 [arXiv:2111.06912] [INSPIRE].

[150] E.K. Morvan, J.P. van der Schaar and M.R. Visser, *On the Euclidean action of de Sitter black holes and constrained instantons*, SciPost Phys. **14** (2023) 022 [arXiv:2203.06155] [INSPIRE].

JHEP05(2024)016